Q3
SJR 2022
0.22

Journal of Degraded and Mining Lands Management

http://www.jdmlm.ub.ac.id

Accredited (SINTA-1) by Ministry of Education, Culture, Research and Technology of Indonesia

Indexed by Asean Citation Index, CABI, ProQuest, Scopus

p-ISSN: 2339-076X
e-ISSN: 2502-2458

Vol 11 No 3 (April 2024)

Research Centre for the Management of Degraded and Mining Lands, and Soil Department, Faculty of Agriculture, Brawijaya University
http://ircmedmind.ub.ac.id, http://tanah.ub.ac.id

Editorial Team

Laman: https://jdmlm.ub.ac.id/index.php/jdmlm/about/editorialTeam

Editorial Team

Editor-in-Chief

Eko Handayanto, Research Centre for the Management of Degraded and Mining Lands, Brawijaya University, Indonesia

Associate Editor-in-Chief

Christopher W Anderson, School of Agriculture and Environment, Massey University, New Zealand

Reni Ustiatik, Research Centre for the Management of Degraded and Mining Lands, Brawijaya University, Indonesia

Sri Rahayu Utami, Department of Soil, Faculty of Agriculture, Brawijaya University, Indonesia

Wani Hadi Utomo, Department of Soil, Faculty of Agriculture, Brawijaya University, Indonesia

Editorial Board

Anizan Isahak, Faculty of Science and Technology, School of Environmental and Natural Resource Sciences, Universiti Kebangsaan Malaysia, Malaysia

Baiq Dewi Krisnayanti, United Nations Development Programme, Jakarta, Indonesia

B M Kumar, College of Forestry, Kerala Agricultural University, India

Constantinos Ehaliotis, Department of Natural Resources and Agricultural Engineering, Agricultural University of Athens, Greece

Gusti Irya Ichriani, Department of Soil, Faculty of Agriculture, Lambung Mangkurat University, South Kalimantan, Indonesia

Hamdan Jol, Department of Land Management, Faculty of Agriculture, Universiti Putra Malaysia, Malaysia

Jianxu Wang, State Key Laboratory of Environmental Geochemistry, Chinese Academy of Sciences, Guiyang, China

John Bako Baon, Indonesian Coffee and Cocoa Research Institute, Jember, Indonesia

Reginawanti Hindersah, Department of Soil Science, Faculty of Agriculture, Universitas Padjadjaran, Indonesia

Editorial Team (lanjutan)

Laman: https://jdmlm.ub.ac.id/index.php/jdmlm/about/editorialTeam

Suhartini S, Department of Agricultural Economics, Faculty of Agriculture, Brawijaya University, Indonesia

Syahrul Kurniawan, Department of Soil, Faculty of Agriculture, Brawijaya University, Indonesia

Technical Editor

Achmad Riyanto, Department of Soil Science, Faculty of Agriculture, Brawijaya University, Indonesia

Christanti Agustina, Department of Soil, Faculty of Agriculture, Brawijaya University, Indonesia

Nina Dwi Lestari, Department of Soil, Faculty of Agriculture, Brawijaya University, Indonesia

Rizki Trisnadi, Brawijaya University, Indonesia

Daftar Isi

Laman: https://jdmlm.ub.ac.id/index.php/jdmlm/issue/view/48

Assessing karst landscape degradation based on the void development of karst aquifers in Gunungsewu, Indonesia

Muhammad Naufal , Tjahyo Nugroho Adji , Eko Haryono , Ahmad Cahyadi — 5707-5715

PDF

DOI : 10.15243/jdmlm.2024.113.5707

Abstract View : 9

PDF downloads: 0

Hydrological function of rewetted peatlands linked to saturated hydraulic conductivity in Kubu Raya, West Kalimantan, Indonesia

Rabbirl Yarham Mahardika , Suria Darma Tarigan , Dwi Putro Tejo Baskoro , Vinni Lovita , Adi Gangga , Adibtya Asyhari , Arif Fatoni , Kristoporus Jepri , Adzan Pandu Ravelle — 5717-5725

PDF

DOI : 10.15243/jdmlm.2024.113.5717

Abstract View : 11

PDF downloads: 5

Estimated changes in carbon stock due to changes in land use around Yogyakarta International Airport

Westi Utami , Catur Sugiyanto , Noorhadi Rahardjo — 5727-5740

PDF

DOI : 10.15243/jdmlm.2024.113.5727

Abstract View : 8

PDF downloads: 5

Elemental composition and mineralogical characteristics of volcanic ash and soil affected by the eruption of Mount Semeru, East Java

Tri Candra Setiawati , Mohammad Nurcholis , Basuki Basuki , Subhan Arif Budiman , Dwi Fitri Yudiantoro — 5741-5753

PDF

DOI : 10.15243/jdmlm.2024.113.5741

Abstract View : 9

PDF downloads: 0

Production of activated carbon from coal with H3PO4 activation for adsorption of Fe(II) and Mn(II) in acid mine drainage

Suliestyah Suliestyah , Edy Jamal Tuheteru , Ririn Yulianti , Christin Palit , Caroline Claudia Yomaki , Shahrul Nizam Ahmad — 5755-5765

PDF

DOI : 10.15243/jdmlm.2024.113.5755

Abstract View : 14

PDF downloads: 7

Changes in properties of reclaimed-mine soil, plant growth, and metal accumulation in plants with application of coal fly ash and empty fruit bunches of oil palm

Akhmad Rizalli Saidy , Bambang Joko Priatmadi , Meldia Septiana , Ratna Ratna , Ismet Fachruzi , Hairil Ifansyah , Afiah Hayati , Muhammad Mahbub , Abdul Haris — 5767-5778

PDF

DOI : 10.15243/jdmlm.2024.113.5767

Abstract View : 13

PDF downloads: 4

Scimago Journal & Country Rank (SJR) Rank

Laman: https://www.scimagojr.com/journalsearch.php?q=21100979353&tip=sid&exact=no

Journal of Degraded and Mining Lands Management

COUNTRY

Indonesia

Universities and research institutions in Indonesia

Media Ranking in Indonesia

SUBJECT AREA AND CATEGORY

Environmental Science
- Management, Monitoring, Policy and Law
- Nature and Landscape Conservation
- Pollution

Social Sciences
- Geography, Planning and Development

PUBLISHER

Brawijaya University

H-INDEX

7

PUBLICATION TYPE

Journals

ISSN

25022458, 2339076X

COVERAGE

2019-2022

INFORMATION

Homepage

How to publish in this journal

editor.jdmlm@ub.ac.id

Peringkat SINTA

Laman: https://sinta.kemdikbud.go.id/journals/profile/920

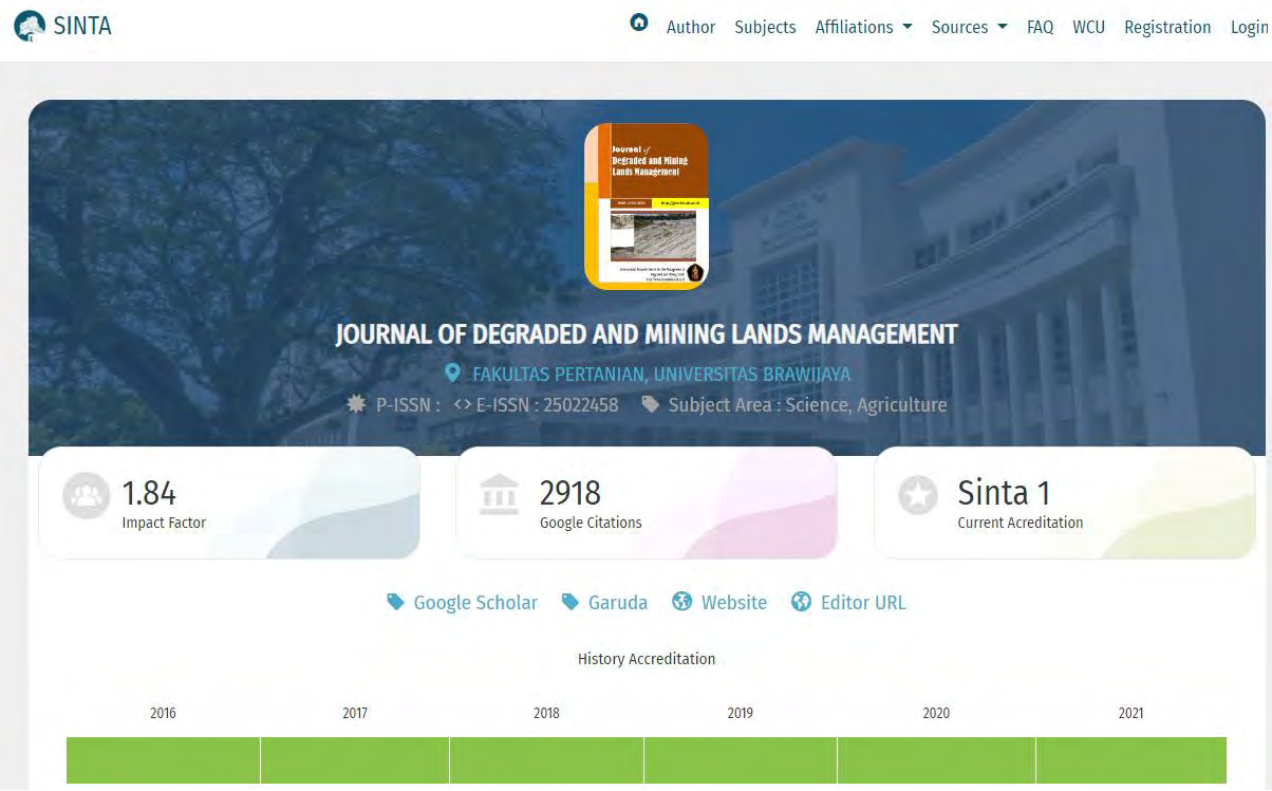

SERTIFIKAT

Kementerian Riset dan Teknologi/
Badan Riset dan Inovasi Nasional

RISTEK-BRIN

Petikan dari Keputusan Menteri Riset dan Teknologi/
Kepala Badan Riset dan Inovasi Nasional
Nomor 200/M/KPT/2020
Peringkat Akreditasi Jurnal Ilmiah Periode III Tahun 2020
Nama Jurnal Ilmiah

Journal of Degraded and Mining Lands Management

E-ISSN: 25022458

Penerbit: Fakultas Pertanian, Universitas Brawijaya, Malang

Ditetapkan sebagai Jurnal Ilmiah

TERAKREDITASI PERINGKAT 1

Akreditasi Berlaku selama 5 (lima) Tahun, yaitu
Volume 7 Nomor 4 Tahun 2020 sampai Volume 12 Nomor 3 Tahun 2025

Jakarta, 23 Desember 2020

Menteri Riset dan Teknologi/
Kepala Badan Riset dan Inovasi Nasional
Republik Indonesia,

Bambang P. S. Brodjonegoro

JOURNAL OF DEGRADED AND MINING LANDS MANAGEMENT
Volume 11, Number 3 (April 2024):5755-5765, doi:10.15243/jdmlm.2024.113.5755
ISSN: 2339-076X (p); 2502-2458 (e), www.jdmlm.ub.ac.id

Research Article

Production of activated carbon from coal with H_3PO_4 activation for adsorption of Fe(II) and Mn(II) in acid mine drainage

Suliestyah[1], Edy Jamal Tuheteru[1*], Ririn Yulianti[1], Christin Palit[1], Caroline Cludia Yomaki[1], Shahrul Nizam Ahmad[2]

[1] Department of Mining Engineering, Faculty of Earth and Energy Technology, Universitas Trisakti, Jl. Kyai Tapa, No. 1, Jakarta Barat 11440, Indonesia
[2] School of Chemistry and Environment, Faculty of Applied Sciences, Universiti Teknologi MARA, Shah Alam, Selangor, Malaysia

[*]corresponding author: ejtuheteru@trisakti.ac.id

Article history:
Received 26 September 2023
Revised 5 February 2024
Accepted 18 February 2024

Keywords:
acid mine drainage
activated carbon
adsorption
carbonization
iodine number

Abstract

Acid Mine Drainage (AMD) contains Fe(II) and Mn(II) metals, which can cause environmental pollution. This research aimed to investigate the potency of activated carbon made from coal as an adsorbent in AMD treatment. The carbon was made of coal and activated with H_3PO_4 in a weight ratio of 40%, 800°C for 120 minutes while supplying 1.5 L/min of nitrogen during the carbonization process. The result shows that BET surface area, total pore volume, and iodine number were 296.4 m^2/g, 0.156 cc/g, and 1,205 mg/g, respectively. The surface contained many fractures, channels, and big holes, as evidenced by the FT-IR and SEM investigations, and it also had acidic surface functional groups. The optimum contact time adsorption for AMD treatment was 30 minutes, and the first concentration of Fe(II) and Mn(II) metals affected the adsorption. The optimum removal of Fe(II) in AMD treatment was 95.27% at an initial concentration of 3.51 ppm, while the optimum removal of Mn(II) was 99.82% at an initial concentration of 5.71 ppm. This activated carbon has a considerable potency to be used as the adsorbent in AMD treatment to reduce Fe(II) and Mn(II) levels.

To cite this article: Suliestyah, Tuheteru, E.J., Yulianti, R., Palit, C., Yomaki, C.C. and Ahmad, S.N. 2024. Production of activated carbon from coal with H_3PO_4 activation for adsorption of Fe(II) and Mn(II) in acid mine drainage. Journal of Degraded and Mining Lands Management 11(3):5755-5765, doi:10.15243/jdmlm.2024.113.5755.

Introduction

The acid mine drainage (AMD) that is formed can have an impact on physical, chemical, biological, ecological, and socio-economic conditions. AMD has a pH range of 2 to 5 and can result from coal mining activities such as removing overburden, coal excavation, and material washing because water and oxygen present cause sulfide minerals to oxidize into sulfuric acid (Kefeni et al., 2017; Skousen et al., 2019). Besides having a low pH, AMD contains heavy metal ions such as Fe, Mn, Cd, Co, Zn, and Ni due to the interaction of AMD with various types of mineral ores (Akcil and Koldas, 2006; García-Valero et al., 2020). Under chemical conditions, there is an increase in heavy metals in surface water and groundwater (Acharya and Kharel, 2020). AMD that is directly discharged into the environment can cause water pollution, corrosion of mining equipment, and damage the balance of aquatic ecosystems (Indra et al., 2014). This pollution condition can have a bad impact on the surrounding environment if AMD is not managed properly. Actions to prevent the formation of AMD have been attempted, one of which is the application of encapsulation. However, the formation of AMD cannot be avoided, so efforts need to be made to treat AMD in various forms, both through active and passive processing (Nishimoto et al., 2021).

CC BY-NC 4.0 | Attribution-NonCommercial 4.0 International

This research was carried out on a laboratory scale to see the potential for AMD treatment by using activated carbon adsorbents to minimize the impact of AMD on the surrounding environment, especially on land around the mining area.

Various methods have been carried out in processing AMD to meet the standard of mine waste, where the pH is between 6 and 8, the TSS content is ≤200 ppm, the Fe(II) metal content is ≤7 ppm and the Mn(II) metal content is ≤4 ppm (Regulation of the Ministry of Environment no 113, 2003). A method to reduce Fe(II) and Mn(II) metals in AMD waste is the use of adsorbents such as activated carbon, which has a large surface area, a regular pore structure, and functional groups on the surface, allowing the adsorption process (Kaur et al., 2018). Numerous raw materials with high carbon content can be used to produce activated carbon, namely coconut shells (Jibril et al., 2013; Liang et al., 2020), palm shells (Ibrahim et al., 2014), coffee grounds (Pagalan et al., 2019), oleaster (Yagmur et al., 2020), biomass (Abioye and Ani, 2017; Ahmed et al., 2019), rubber seed shell (Sun and Jiang, 2010), sawdust (Intan et al., 2016), fluted pumpkin stem waste (Ekpete and Horsfall, 2011), peanut shells and rice husk (Ragadhita and Nandiyanto, 2021), honeydew peel (Yunus et al., 2015), oil palm empty fruit bunch wastes (Wirasnita et al., 2015) and candlenut shell (Nandiyanto et al., 2023). However, the resources are limited, which renders it difficult to meet the need to synthesize activated carbon at an industrial scale.

The use of low-rank coal, having abundant and easily accessible reserves, is required to get the activated carbon with high adsorption properties that can be applied on an industrial scale. The activated carbon from the coal has been produced using various activation and surface modification techniques and has been applied as an adsorbent. Monika (2017) has made activated carbon from coal by activating a mixture of KOH and NaOH to adsorb CO gas. Anbia and Amirmahmoodi (2016) modified the surface of coal-activated carbon using surfactants to adsorb Hg and Mn(II) metals. Coal has been used in the production of activated carbon by Li et al. (2018) and Li et al. (2020), which produces highly effective Fe(II) dye adsorbent.

The activated carbon made from coal has the potency to be adsorbent in AMD processing to reduce Fe(II) and Mn(II) levels of metals. The carbon itself has been activated using $ZnCl_2$, and its application in liquid waste can adsorb Fe(II) metal by 96% (Suliestyah et al., 2020a). The adsorption of coal-activated carbon with $ZnCl_2$ activation on Fe(II) and Mn(II) metals in AMD has been carried out, which resulted in the adsorption of 99.7-100% Fe(II) and 26.5–56 Mn(II)% (Suliestyah et al., 2020b), (Suliestyah et al., 2021a). The results showed that coal-activated carbon has a high adsorption capacity for Fe(II) metal but is still low for Mn(II) metal. Thus, it is necessary to explore alternative methods, such as the H_3PO_4 activation method, to improve the ability of the activated carbon to adsorb the Mn(II) metal.

The production of activated carbon from coal by activating a mixture of H_3PO_4 and NH_4HCO_3 has been carried out by Kusdarini et al. (2017), which produced a highly effective adsorbent with an iodine number of 1,238.5 mg/g. The production of activated carbon from coal by activating H_3PO_4 has been carried out by Sitorus (2015). The resulting activated carbon can adsorb 38.78% Mn(II) metal in artificial AMD with an initial concentration of 25 ppm at pH 3. The activation of H_3PO_4 in the process of making activated carbon has also been carried out by Esterlita and Herlina (2015), which produces activated carbon with an iodine number of 767.745 mg/g, and Sun et al. (2016), which produced activated carbon with a surface area of 1,252 m^2/g. The object of this study was the manufacture of activated carbon with coal as a raw material, using phosphoric acid for activation. The resulting activated carbon was used as an adsorbent to reduce Fe and Mn metal levels in laboratory-scale acid mine drainage (AMD) treatment.

Materials and Methods

In this research, the production of activated carbon from coal was carried out using H_3PO_4 activation, a mixture of 60% coal and 40% H_3PO_4. The resulting carbon was applied as an adsorbent to Fe(II) and Mn(II) metals in artificial AMD, with the aim of seeing its potential in AMD treatment. Characterization of the activated carbon included proximate quality, iodine number, surface area, surface morphology, and infrared absorption of functional groups on the surface of activated carbon. Laboratory-scale applications used artificial AMD to carry out adsorption tests on Fe(II) and Mn(II) metals.

The coal samples were brought from PT Bukit Asam, Bangko Barat Mining Pit 1 Layer A2 Tanjung Enim, South Sumatra, Indonesia. To remove any moisture that might have been retained during the storage procedure, coal samples that had been prepared to 60 mesh size were put in a drying oven at 105°C for one hour. The samples were chemically activated using 60% coal and 40% H_3PO_4. Afterward, the samples were heated to 800°C in an airtight reactor with nitrogen flowing through it at a rate of 1.5 liters per minute for one hour in order to carbonize them. Next, hot water was used to wash and then dry the activated carbon. The choice of phosphoric acid activator is because this compound has high thermal stability and covalent character, so it is expected to increase adsorption and maximize activated carbon's potential as an adsorbent. This phosphoric acid functions to bind non-carbon impurity compounds so that the pores on the carbon will be more open (Lestari et al., 2016).

Artificial AMD was made from standard solutions containing 1,000 ppm Fe(II) and 1,000 ppm Mn(II). Each solution was diluted with distilled water,

CC BY-NC 4.0 | Attribution-NonCommercial 4.0 International

and the dilution results for two concentration variations of each solution were mixed and measured by applying AAS method for setting the concentration of Fe(II) and Mn(II); this solution was an artificial AMD. AMD samples were taken from the coal mining site of PT Banjarsari Pribumi, in the Banjarsari area, Lahat Regency, South Sumatra, Indonesia. Coal samples were taken from the mining site at Bangko Barat Mining, PT Bukit Asam, Tanjung Enim, South Sumatra, Indonesia.

In the process of characterizing activated carbon, a scanning electron microscope was used for analyzing the surface morphology (SEM- Jeol JSM-IT200), and using the Surface Area Analyzer (SAA) and Brunauer-Emmett-Teller (BET) technique, surface area, pore volume, and pore diameter were investigated. The surface's functional groups were identified using the Fourier-Transform Infrared Spectroscopy (FT-IR) method. The results of testing for Fe(II) and Mn(II) levels, both before and after activated carbon treatment, were carried out using the Atomic Absorption Spectroscopy (AAS) method. The proximate analysis included moisture content (ASTM D.3173), ash content (ASTM D.3174), volatile matter content (ASTM D.3175), and bound carbon (ASTM D.3172). Meanwhile, the sulfur content used the ASTM D.3177 method, and the calorific value used the ASTM D.5685 method.

Adsorption capacity was measured by the iodine number. Utilizing the activated carbon that had been baked in an oven, weighted up to 0.5 g, and placed in an erlenmeyer, the amount of iodine that could be adsorbed was determined. Iodine 0.1 N solution of 50 mL was applied to the sample, which was then left for 15 minutes while being shaken. Then, 10 mL of the filtrate was collected and titrated with a 0.1 N $Na_2S_2O_3$ solution. The iodine number was determined using ASTM D4607-94 method.

Activated carbon adsorption testing was carried out on a laboratory scale using artificial AMD and AMD samples taken from coal mining sites. Two grams of activated carbon were combined with 200 mL of artificial AMD and AMD samples in a different container. Then, this mixture is put into a shaker that is set to 150 rpm and 25°C. The contact time used could be anywhere between 30, 60, 90, 120, and 150 minutes. The study examined how contact time affects the elimination of the metals Fe(II) and Mn(II). The AAS was used to compare the concentration of metal ions in AMD before and after adsorption in order to assess the ability of activated carbon to get rid of Fe(II) and Mn(II) ions.

The quality of the coal used as a raw material was assessed. Table 1 shows the results of the proximate analysis, calorific value, and sulfur. Based on the finding in Table 1, the coal used to make activated carbon has Sub-Bituminous B quality.

Based on the result of dilution in the standard Fe(II) and Mn(II) solutions, two initial concentrations were obtained, which can be seen in Table 2, which shows the initial concentration in artificial AMD before treatment using activated carbon.

Table 1. Results of the analysis of coal quality.

No	Analysis Parameters	Analysis Results
1	Moisture (%, adb)	12.85
2	Ash (%, adb)	1.305
3	Volatile Matter (%, adb)	41.7256
4	Fixed Carbon (%, adb)	44.1194
5	Total Sulfur (%, adb)	0.095
6	Calorific Value (cal/g, adb)	5,445.06

Table 2. Initial concentrations of Fe(II) and Mn(II).

No	Concentration	Sample 1	Sample 2
1	Fe(II)	18.88	38.11
2	Mn(II)	11.00	18.77

From the coal mining site of PT Banjarsari Pribumi, in the Banjarsari area, Lahat Regency, South Sumatra Indonesia, the initial concentration of Fe(II) and Mn(II) is presented in Table 3.

Table 3. Initial concentrations of Fe(II) and Mn(II) from the coal mining site.

No	Fe(II) and Mn(II)	Concentration (ppm)
1	Fe(II)	3.51
2	Mn(II)	5.71

Result and Discussion

The iodine number is a parameter that shows the adsorption capacity of the activated carbon with an increase in pore size and surface area. New pores develop on the coal surface as a result of the carbonization process, and the activation of the acid prevents the formation of tar, which can close the pores. Phosphoric acid, which is hygroscopic, absorbs water in the coal before the carbonization process (Verayana et al., 2018). Table 4 shows the iodine number of coal, the activated carbon from coal without chemical activation, and the activated carbon from coal with H_3PO_4 activation. In Table 4, it appears that carbonization of coal can significantly increase the iodine from 310 mg/g to 1,043 mg/g, and activation of H_3PO_4 can increase the iodine from 1,043 mg/g to 1,206 mg/g. Activation with H_3PO_4 in this study resulted in a higher iodine number compared to the activated carbon made by Sun et al. (2016) (645 mg/g), Kurniawan et al. (2014) (219 mg/g) and by Yunus et al. (2015) (734-942 mg/g) which used coconut shell as raw material, and by Husin et al. (2020) (1,080 mg/g) which used durian peel as raw material. Table 5 shows a comparison between iodine number and proximate analysis compared to the quality standard of activated carbon based on SNI 06-3730-1995.

CC BY-NC 4.0 | Attribution-NonCommercial 4.0 International

Table 4. Iodine number.

No	Sample Type	Iodine Number (mg/g)
1	Coal	310
2	Activated carbon without chemical activation	1,043
3	Activated carbon with chemical activation of H_3PO_4	1,205

As shown in Table 5, the moisture, ash, and volatile matter content have decreased, compared to those in coal (Table 1), because the carbonization process at a temperature of 800°C has removed most of the moisture and volatile matter content in the coal. Table 5 shows that water content, ash content, and iodine numbers meet the standards for activated carbon as regulated in SNI 06-3730-1995. However, the volatile matter and bound carbon content do not meet this standard, for the time for carbonization is only 1 hour.

Table 5. Comparison of activated products with standards

No	Parameter	Activated carbon with H_3PO_4 activation	Quality Standard of Activated Carbon SNI 06-3730-1995
1	Moisture (%, adb)	9.1	Max 15
2	Ash (%, adb)	1.33	Max 10
3	Volatile Matter (%, adb)	30.3	Max 25
4	Fixed Carbon (%, adb)	59.3	Min 65
5	Iodine Number	1,205	750

Table 6 shows the BET surface area, total pore volume, and average pore diameter of the coal-derived activated carbons. The outcomes demonstrate its effectiveness as an activating agent to create the activated carbons with a high surface area and porosity. The activated carbons were carbonized using H_3PO_4 to improve their surface area and porous structure.

Table 6. Surface area, total volume, and pore radius.

No	Sample	Surface area (m^2/g)	Total Pore Volume (cc/g)	Average Pore Radius (Å)
1	Coal	2.78	0.004	27.32
2	Activated carbon activated by H_3PO_4	296.4	0.156	10.54

Activation with H_3PO_4 in this study resulted in a higher BET surface area compared to the activated carbon made by Husin and Hasibuan (2020) (44.3 m^2/g) and by Retno et al. (2016) (61.8 m^2/g) but lower BET surface area compared to the activated carbon made by Kurniawan et al. (2014) (386 m^2/g). Table 6 shows a noticeable increase in surface area from 2.78 m^2/g (raw material coal) to 296.4 m^2/g (activated carbon). The total pore volume also experienced a sharp increase from 0.004 cc/g (coal) to 0.156 cc/g (activated carbon). The surface area of this activated carbon is higher than that of the activated carbon made from durian peels with H_3PO_4 activation of 86.2 m^2/g (Husin and Hasibuan, 2020). The increased surface area of activated carbon is due to the activation process using H_3PO_4, which binds water to H_3PO_4, which is hygroscopic. This water binding can prevent the formation of tar during the carbonization process, so that the pores that are formed are not covered by tar. When more pores are formed, they will expand the surface of the activated carbon (Kurniawan et al., 2014).

A factor that affects the adsorbent's capacity to adsorb is the shape of the pore surface. The pores contained in activated carbon can increase adsorption because these pores are gaps that expand the surface of activated carbon. The coal and activated carbon from coal with the highest surface area were exposed to the SEM to investigate the surface morphology of the samples. The SEM images of the coal and the activated carbon are shown in Figures 1 and 2. The surface morphology of the coal and the activated carbon sample differ significantly from one another. Compared to activated carbon, the coal's surface is slightly smoother and has fewer Fe(II) cavities and fissures. According to the BET surface area value (2.8 m^2/g), it can be shown that the coal has a thick wall structure and only a small amount of porosity (Figure 1). This is because most of the pores in coal are still covered by hydrogen, tar, and other compounds consisting of ash, water, nitrogen, and sulfur. After the activation and carbonization processes, the raw material's thick wall opened up, and the result was a broader porosity in relation to the increase in surface area to 296.4 mg/g (Figure 2). Surface functional groups on the activated carbon were studied through FT-IR analysis (Figure 3). The FT-IR spectra of coal and activated carbon are displayed in Figures 1 and 2. After the activation, several of the prominent peaks seen in the coal vanished. In particular, it was found that the intensities of the 1,639-1,587/cm C–C stretching vibrations in aromatic ring bands and the 2,916-2,850/cm aliphatic C–H vibrations were decreased. This condition might have a relation to the activation-induced breakdown of cellulose, hemicellulose, and lignin in the coal. The presence of

CC BY-NC 4.0 | Attribution-NonCommercial 4.0 International

the OH stretching vibration of alcohol, phenol, or carboxylic acid is indicated by the broad and flat band at 3,300-3,400/cm. C-H stretching is represented by the faint peaks at 1,289/cm. Functional groups on the surface of this activated carbon have free electrons, allowing the bonding with metal ions to occur, thereby reducing the levels of Fe(II) and Mn(II) metals in the waste (Kiliç et al., 2012; Husin and Hasibuan, 2020).

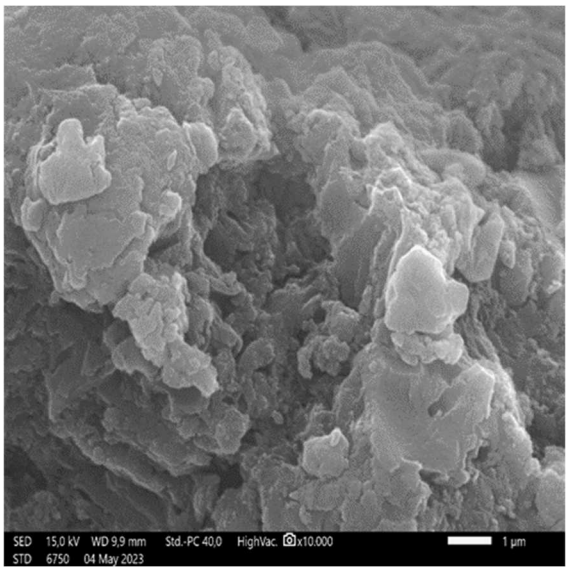

Figure 1. SEM of coal.

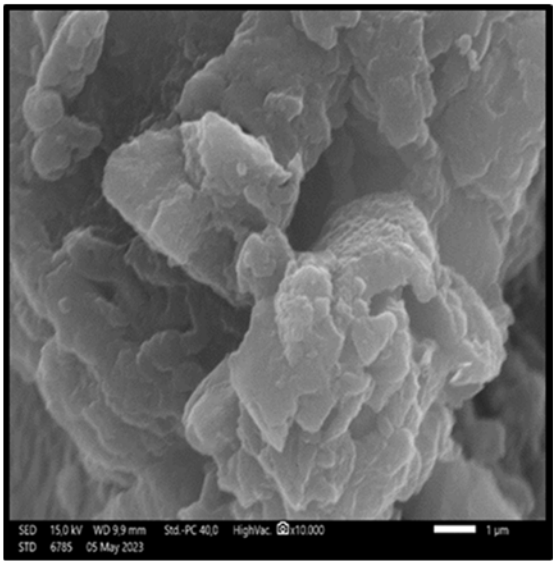

Figure 2. SEM of activated carbon.

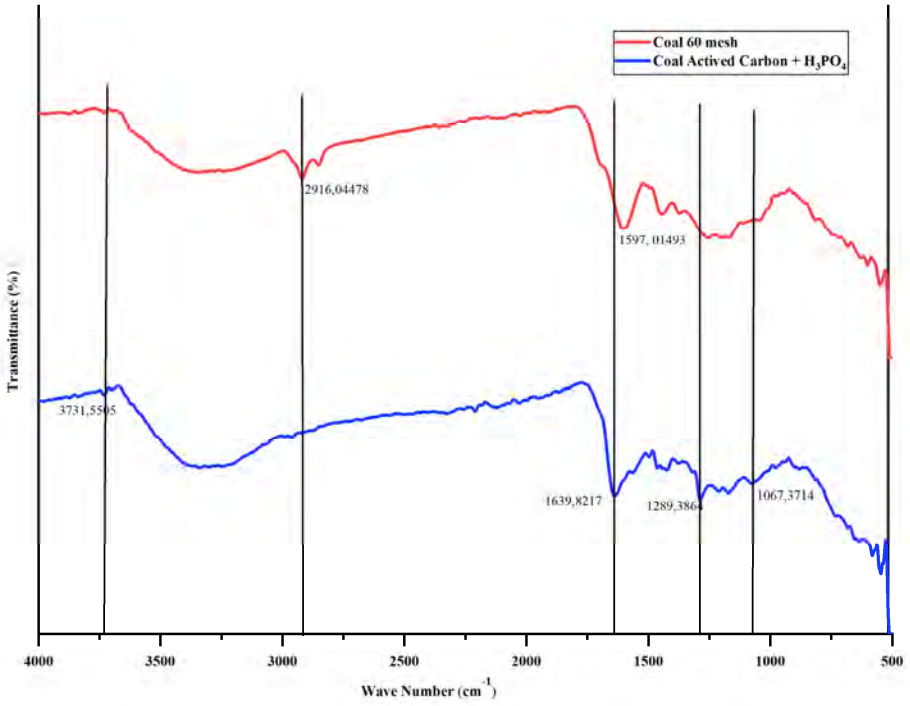

Figure 3. FT-IR of coal and activated carbon.

Table 7 shows the changes in the concentration of Fe(II) metal with initial concentrations 18.88 ppm and 38.11 ppm. Data at 0 minutes is the initial condition, and adsorption occurs at various contact times of 30, 60, 90, 120, and 150 minutes. The data in Table 7 is depicted as a graph of the reduction in Fe(II) concentration in Figure 4 and the percentage of Fe(II) uptake by activated carbon in Figure 5. Figure 4 shows that the Fe(II) removal occurs at 30 to 150 minutes. A very sharp decrease in the curve occurred at 30

CC BY-NC 4.0 | Attribution-NonCommercial 4.0 International

minutes, which showed a significant decrease in Fe(II) concentration, where at an initial concentration of 18.88 ppm, it fell to 1.15 ppm (93.9% decrease), and at an initial concentration of 38.11 ppm, it fell to 10.97 ppm (71.2% decrease). After 30 to 150 minutes, the curve appeared to be sloping, which indicated that Fe(II) removal was not significant. At an initial concentration of 18.88 ppm, the maximum removal occurred at 150 minutes at 94.9%, and for an initial concentration of 38.11 ppm, it occurred at 150 minutes at 75.29%. The percentage of Fe(II) removal is shown in Figure 5.

Table 7. The Fe(II) removal after adsorption.

Contact time of adsorption (minutes)	0	30	60	90	120	150
Concentration of sample 1 (ppm)	18.88	1.15	1.14	1.1	0.97	0.95
Concentration of sample 2 (ppm)	38.11	10.97	10.618	9.819	9.98	9.41

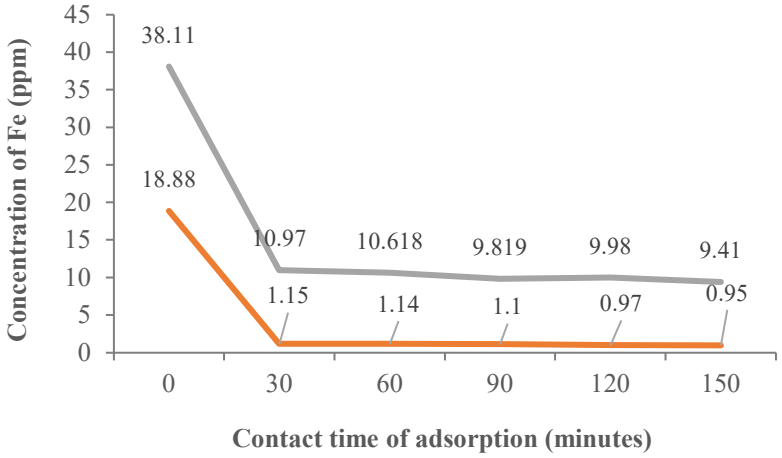

Figure 4 Reduction of Fe(II) concentration.

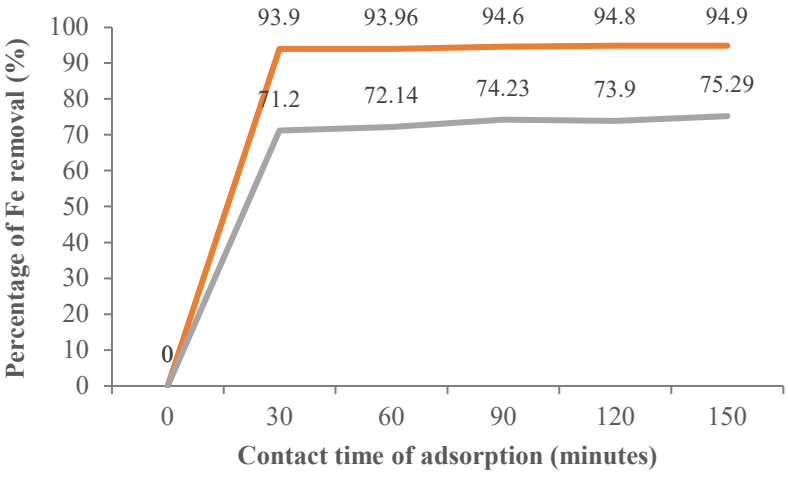

Figure 5. Percentage of Fe(II) removal.

At a lower initial concentration (18.88 ppm), the percentage of Fe(II) adsorption ranged from 93.9-94.9%, but at a higher initial concentration (38.11 ppm), the percentage of Fe(II) adsorption decreased to around 71.2-75.29%. Table 8 shows the changes in the concentration of Mn(II) metal with the initial concentrations of 11 ppm and 18.77 ppm. Data at 0 minutes is the initial condition, and adsorption occurs at various contact times of 30, 60, 90, 120, and 150 minutes. The data in Table 8 is depicted as a graph of the reduction in Mn(II) concentration in Figure 6 and the percentage of Fe(II) uptake by activated carbon in Figure 7. Figure 6 shows the concentration of Mn(II) ions in ppm units. At minute 0, the initial concentration

CC BY-NC 4.0 | Attribution-NonCommercial 4.0 International

before the adsorption of activated carbon occurs. Mn(II) removal occurs at 30 to 150 minutes. There are two curves of decreasing Mn(II) concentration with different initial concentrations. A very sharp decrease in the curve occurred at 30 minutes, which showed a significant decrease in Mn(II) concentration, in which an initial concentration at 11 ppm led to the decrease to 4.66 ppm (57.63% decrease), and at the first concentration of 18.77 ppm, it decreased into 9.51 ppm (49.26% decrease). After 30 to 150 minutes, the curve appeared to be sloping, which indicated that Mn(II) removal was not significant. At the first concentration of 11 ppm, the maximum removal occurred at 120 minutes at 65.54%. Meanwhile, for an initial concentration of 18.77 ppm, it occurred at 150 minutes at 50.38%.

Table 8. The Mn(II) removal after adsorption.

Concentration	Contact time of adsorption (minutes)					
	0	30	60	90	120	150
Concentration of sample 1 (ppm)	11	4.66	4.64	4.7164	3.7979	4.6927
Concentration of sample 2 (ppm)	18.77	9.51	9.34	9.35	9.44	9.3

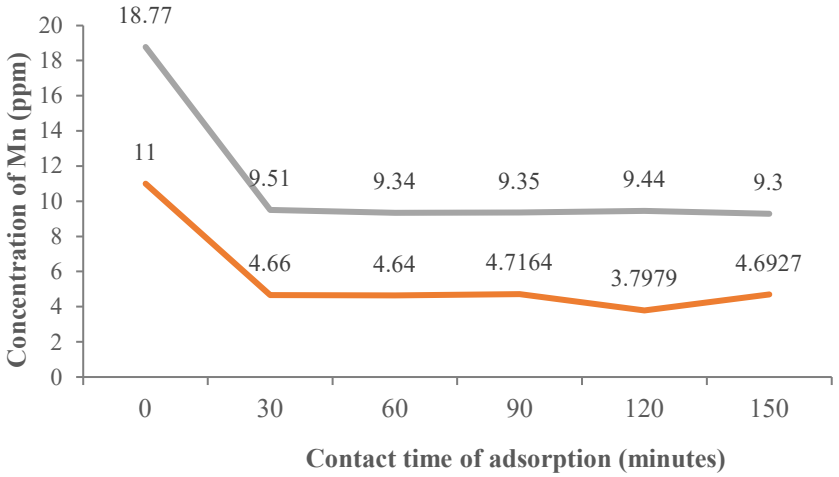

Figure 6. Reduction of Mn(II) concentration.

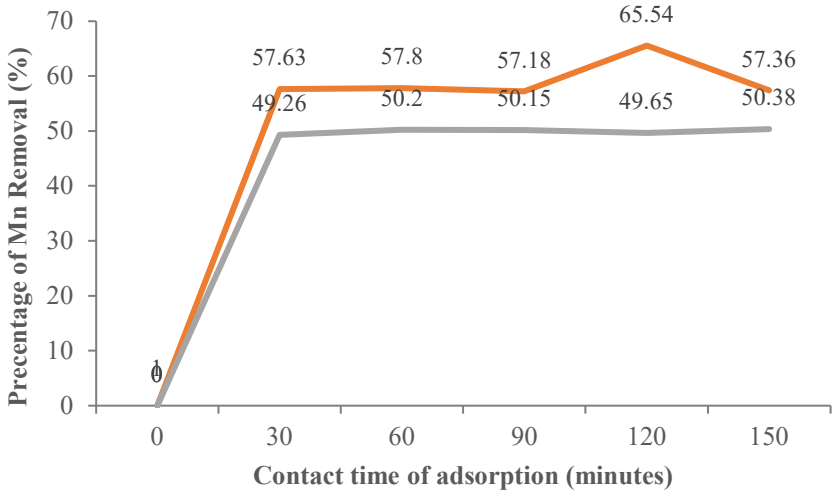

Figure 7. Percentage of Mn(II) removal.

CC BY-NC 4.0 | Attribution-NonCommercial 4.0 International

The percentage of Fe(II) removal is shown in Figure 7. The percentage of Mn(II) adsorption varied between 57.18 and 65.54% at a lower initial concentration (11 ppm) but reduced to roughly 49.26 to 50.38 percent at a higher initial concentration (18.77 ppm). This study shows that the activated carbon treatment on artificial AMD is proven effective for reducing Fe(II) and Mn(II) metals. Figures 5-7 indicate that the most effective contact time in the adsorption process was 30 minutes, which resulted in the greatest percentage of Fe(II) and Mn(II) removal. Therefore, this study continued with the activated carbon treatment on AMD samples collected from the coal mining site of PT Banjarsari Pibumu, South Sumatra (Table 9).

Table 9. The Fe(II) and Mn(II) removal after adsorption.

Concentration	Contact time (minutes)					
	0	30	60	90	120	150
Concentration of Fe(II)	3.51	0.16	0.17	0.17	0.15	0.16
Concentration of Mn(II)	5.71	0.01	0.006	0.007	0.005	0.008

Table 9 shows the changes in the concentration of Fe(II) and Mn(II) metal in the initial conditions before treatment (0 minutes) and the concentration left in AMD after adsorption by activated carbon with the contact times of 30, 60, 90, 120, and 150 minutes. The data in Table 9 is depicted as a graph of the reduced concentration of Fe(II) and Mn(II) in Figure 8 and the percentage of Fe(II) and Mn(II) uptake by activated carbon in Figure 9. Figure 8 shows the concentration of Fe(II) and Mn(II) ions in ppm units in AMD from the coal mining site. A very sharp decrease in the curve occurred at 30 minutes, which showed a significant decrease in Fe(II) concentration, where from an initial concentration of 3.51 ppm Fe(II) to 0.166 ppm (95% decrease).

At an initial Mn(II) concentration of 5.71 ppm, Fe(II) decreased to 0.01 ppm (99.8% decrease). After 30 to 150 minutes, the curve appeared to be sloping, which indicated that Fe(II) and Mn(II) removal was not significant. For Fe(II) removal, the maximum removal occurred at 120 minutes at 95.72%, and for Mn(II) removal, it occurred at 60 minutes at 99.89%. The percentage of Fe(II) and Mn(II) removal is shown in Figure 9.

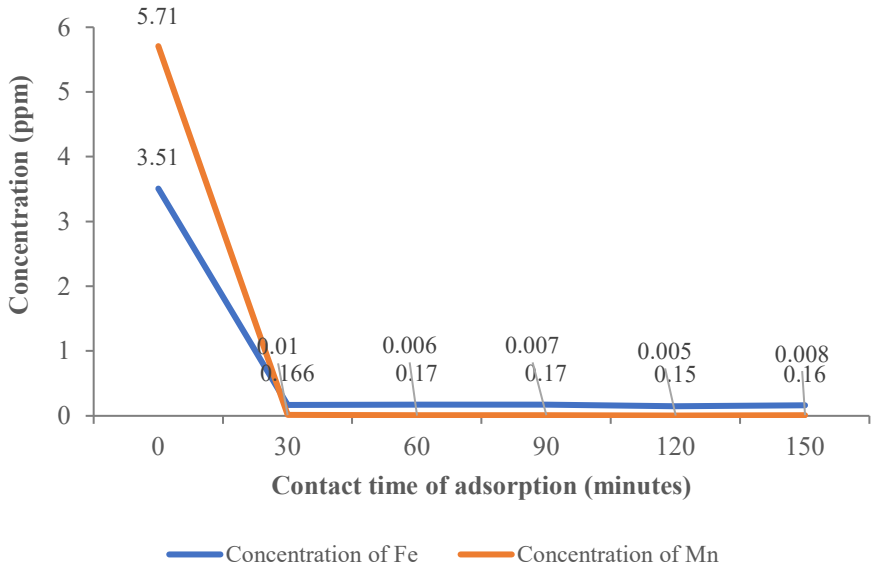

Figure 8. Reduction of Fe(II) and Mn(II).

In artificial AMD treatment with high concentrations of Fe(II) and Mn(II), the Fe(II) removal is more effective than that of Mn(II). The adsorption capacity will increase with increasing electronegativity. Because the charge on the Fe(II) ion drew more strongly toward the atomic nucleus than the Mn(II) ion did in the electron orbital, Fe(II) has a smaller ionic radius than Mn(II. The microporous nature of the activated carbon utilized makes it easier for tiny metal ions to become trapped inside its pores. Treatment of AMD from coal mining sites shows that the Fe(II) and Mn(II) removal do not differ significantly because the initial concentrations of Fe(II) and Mn(II) are low. In all AMD treatment trials with the use of activated carbon, the first concentration affected the adsorption capacity, in which higher initial concentrations of Fe and Mn led to a lower percentage of adsorption. This is because the activated carbon surface has a certain

CC BY-NC 4.0 | Attribution-NonCommercial 4.0 International

adsorption capacity for each metal. If metal adsorption has reached its maximum capacity, the adsorption process decreases. In comparison to the earlier research, which included the adsorption of Fe(II) of 85.32% (Sianipar et al., 2016), 96.24% (Suliestyah et al., 2020a), and 98.23% (Suliestyah et al., 2021b), this study produced almost the same adsorption of Fe(II) (95.7%).

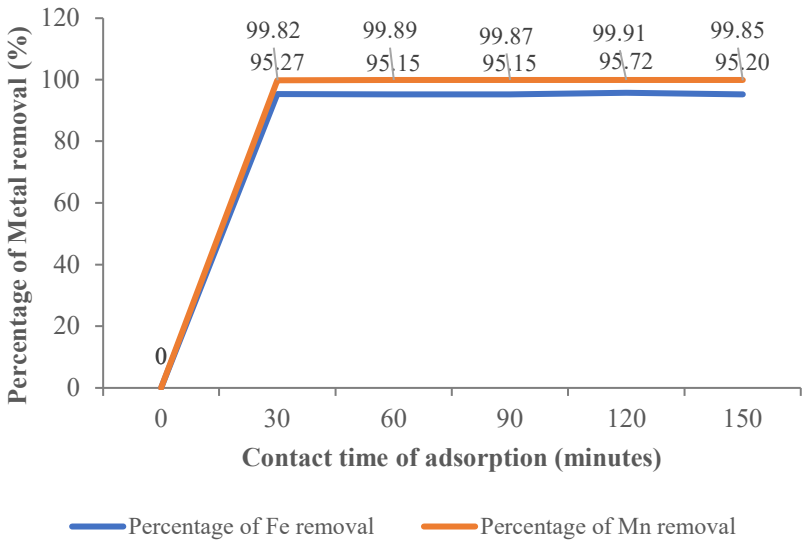

Figure 9. Percentage of Fe(II) and Mn(II).

The result of this study's Mn(II) adsorption (99.9%) was greater than that of earlier research, which reported Mn(II) absorption of 26.3% (Suliestyah et al., 2021a), 56% (Suliestyah et al., 2020b) and 92.89% (Sitorus, 2015), respectively. This study showed that the activated carbon made from coal with H_3PO_4 activation has a high adsorption capacity for Fe(II) and Mn(II) metals in artificial AMD waste, thus having a potency to be used as an adsorbent in AMD treatment.

Conclusion

The characterization of activated carbon with H_3PO_4 activation revealed that the BET surface area, total pore volume, and iodine number were 296.4 m^2/g, 0.1562 cc/g, and 1206 mg/g, respectively. The FT-IR and SEM analyses showed that the surface had acidic surface functional groups and was extremely porous, with numerous fractures, channels, and sizable holes. Treatment of activated carbon in artificial AMD showed that adsorption was affected by the initial concentration of Fe(II) and Mn(II) metals. The greater the initial concentration of Fe(II) and Mn(II), the lower the adsorption power of activated carbon. The results showed that AMD adsorption treatment using H_3PO_4 activated carbon was achieved at 30 minutes of the optimum contact time, with a percentage of Fe(II) removal of 95.27% and a percentage of Mn(II) removal of 99.82%. The findings of this study suggest that the use of coal-activated carbon with H_3PO_4 activation as an adsorbent in AMD treatment to lower Fe(II) and Mn(II) levels has a very high potential.

Acknowledgments

The authors acknowledge PT Bukit Asam for allowing coal sampling and PT Banjarsari Pribumi for allowing acid mine drainage to be sampled. Thanks are also directed to the BRIN laboratory for assisting in testing BET, SEM, FT-IR, and AAS, and to the Coal Quality Analysis Laboratory for assisting in testing the quality of coal and activated carbon.

References

Abioye, A.M. and Ani, F.N. 2017. Advancement in the production of activated carbon from biomass using microwave heating. *Jurnal Teknologi (Sciences & Engineering)* 79(3):79-88, doi:10.11113/jt.v79.7249.

Acharya, B.S. and Kharel, G. 2020. Acid mine drainage from coal mining in the United States – An overview. *Journal of Hydrology* 588(April):125061, doi:10.1016/j.jhydrol.2020.125061.

Ahmed, M.B., Hasan Johir, M.A., Zhou, J.L., Ngo, H.H., Nghiem, L.D., Richardson, C., Moni, M.A. and Bryant, M.R. 2019. Activated carbon preparation from biomass feedstock: Clean production and carbon dioxide adsorption. *Journal of Cleaner Production* 225:405-413, doi:10.1016/j.jclepro.2019.03.342.

Akcil, A. and Koldas, S. 2006. Acid Mine Drainage (AMD): causes, treatment and case studies. *Journal of Cleaner Production* 14(12-13 SPEC. ISS.):1139-1145, doi:10.1016/j.jclepro.2004.09.006.

Anbia, M. and Amirmahmoodi, S. 2016. Removal of Hg (II) and Mn (II) from aqueous solution using nanoporous carbon impregnated with surfactants. *Arabian Journal of Chemistry* 9:S319-S325, doi:10.1016/j.arabjc.2011.04.004.

Ekpete, O. and Horsfall, M. 2011. Preparation and characterization of activated carbon derived from fluted

CC BY-NC 4.0 | Attribution-NonCommercial 4.0 International

pumpkin stem waste (*Telfairia occidentalis* Hook F). *Research Journal of Chemical Sciences* 1(3):10-17.

Esterlita, M.O. and Herlina, N. 2015. Effect of adding $ZnCl_2$, KOH, and H_3PO_4 activators in making active carbon from sugar palm fronds (*Arenga pinnata*). *Jurnal Teknik Kimia USU* 4(1):47-52, doi:10.32734/jtk.v4i1.1460 (*in Indonesian*).

García-Valero, A., Martínez-Martínez, S., Faz, A., Rivera, J. and Acosta, J.A. 2020. Environmentally sustainable acid mine drainage remediation: Use of natural alkaline material. *Journal of Water Process Engineering* 33(December 2019):101064, doi:10.1016/j.jwpe.2019.101064.

Husin, A. and Hasibuan, A. 2020. Study of the effect of varying phosphoric acid (H_3PO_4) concentration and carbon soaking time on the characteristics of activated carbon from durian peel. *Jurnal Teknik Kimia USU* 9(2):80-86, doi:10.32734/jtk.v9i2.3728 (*in Indonesian*).

Ibrahim, I., Martin, A. and Nasruddin, N. 2015. Manufacture and characterization of activated carbon made from palm shells using the physical activation method using a rotary autoclave. *Jom FTEKNIK* 1(2):1-11 (*in Indonesian*).

Indra, H., Lepong, Y., Gunawan, F. and Abfertiawan, M.S. 2014. Application of active and passive treatment methods in management of Lati site acid mine water. *5th Acid Mine Water and Post-mining Seminar in Indonesia*, November 2014, 1-9 (*in Indonesian*).

Intan, D., Said, I. and Abram, H. 2016. Utilization of sawdust biomass as an absorbent for lead metal. *Jurnal Akademika Kimia* 5(4):166-171 (*in Indonesian*).

Jibril, M., Noraini, J., Poh, L.S. and Evuti, A.M. 2013. Removal of colour from waste water using coconut shell activated carbon (CSAC) and commercial activated carbon (CAC). *Jurnal Teknologi (Sciences and Engineering)* 60(May 2014):15-19, doi:10.11113/jt.v60.1435.

Kaur, G., Couperthwaite, S.J., Hatton-Jones, B.W. and Millar, G.J. 2018. Alternative neutralisation materials for acid mine drainage treatment. *Journal of Water Process Engineering* 22(January):46-58, doi:10.1016/j.jwpe.2018.01.004.

Kefeni, K.K., Msagati, T.A.M. and Mamba, B.B. 2017. Acid mine drainage: Prevention, treatment options, and resource recovery: A review. *Journal of Cleaner Production* 151:475-493, doi:10.1016/j.jclepro.2017.03.082.

Kiliç, M., Apaydin-Varol, E. and Pütün, A.E. 2012. Preparation and surface characterization of activated carbons from *Euphorbia rigida* by chemical activation with $ZnCl_2$, K_2CO_3, NaOH, and H_3PO_4. *Applied Surface Science* 261:247-254, doi:10.1016/j.apsusc.2012.07.155.

Kurniawan, R., Luthfi, M. and Wahyunanto, A. 2014. Characterization of BET (Braunanear, Emmelt and Teller) surface area of activated carbon from coconut shells and empty oil palm fruit bunches with phosphoric acid activation. *Jurnal Keteknikan Pertanian Tropis dan Biosistem* 2(1):15-20 (*in Indonesian*).

Kusdarini, E., Budianto, A. and Ghafarunnisa, D. 2017. Production of activated carbon from bituminous coal with a single activation of H_3PO_4, combination of H_3PO_4-NH_4HCO_3, and thermal. *Reaktor* 17(2):74, doi:10.14710/reaktor.17.2.74-80 (*in Indonesian*).

Lestari, R.S.D., Sari, D.K., Rosmadiana, A. and Dwipermata, B. 2016. Preparation and characterization of coconut shell activated carbon with phosphoric acid activator and its application in the purification of used cooking oil. *Teknika: Jurnal Sains dan Teknologi* 12(2):419, doi:10.36055/tjst.v12i2.6607 (*in Indonesian*).

Li, H., Zheng, F., Wang, J., Zhou, J., Huang, X., Chen, L., Hu, P., Gao, J.M., Zhen, Q., Bashir, S. and Liu, J.L. 2020. Facile preparation of zeolite-activated carbon composite from coal gangue with enhanced adsorption performance. *Chemical Engineering Journal* 390, doi:10.1016/j.cej.2020.124513.

Li, L., Sun, F., Gao, J., Wang, L., Pi, X. and Zhao, G. 2018. Broadening the pore size of coal-based activated carbon: Via a washing-free chem-physical activation method for high-capacity dye adsorption. *RSC Advances* 8(26):14488-14499, doi:10.1039/c8ra02127a.

Liang, Q., Liu, Y., Chen, M., Ma, L., Yang, B., Li, L. and Liu, Q. 2020. Optimized preparation of activated carbon from coconut shell and municipal sludge. *Materials Chemistry and Physics* 241(July 2019)., doi:10.1016/j.matchemphys.2019.122327.

Monika, I. 2017. Potential study of Indonesia coal for adsorbed natural gas. *Indonesian Mining Journal* 19(3):133-142, doi:10.30556/imj.vol19.no3.2016.406.

Nandiyanto, A.B.D., Fiandini, M., Ragadhita, R. and Aziz, M. 2023. How to purify and experiment with dye adsorption using carbon: step-by-step procedure from carbon conversion from agricultural biomass to concentration measurement using UV Vis Spectroscopy. *Indonesian Journal of Science & Technology* 8:363-380.

Nishimoto, N., Yamamoto, Y., Yamagata, S., Igarashi, T. and Tomiyama, S. 2021. Acid mine drainage sources and impact on groundwater at the Osarizawa mine, Japan. *Minerals* 11(9):1-15, doi:10.3390/min11090998.

Pagalan, E., Sebron, M., Gomez, S., Salva, S.J., Ampusta, R., Macarayo, A.J., Joyno, C., Ido, A. and Arazo, R. 2019. Activated carbon from spent coffee grounds as an adsorbent for treatment of water contaminated by aniline yellow dye. *Industrial Crops and Products* 145:111953, doi:10.1016/j.indcrop.2019.111953.

Ragadhita, R. and Nandiyanto, A.B.D. 2021. How to calculate adsorption isotherms of particles using two-parameter monolayer adsorption models and equations. *Indonesian Journal of Science and Technology* 6(1):205-234, doi:10.17509/ijost.v6i1.32354.

Regulation of the Ministry of Environment no 113. 2003. Waste Water Quality Standards for Coal Mining Businesses and Activities (*in Indonesian*).

Sianipar, L.D., Zaharah, T.A. and Syahbanu, I. 2016. Adsorption of Fe(II) with cocoa (*Theobroma cacao* L.) fruit shell charcoal activated by hydrochloric acid. *Jurnal Kimia Khatulistiwa* 5(2):50-59 (*in Indonesian*).

Sitorus, S. 2015. Utilization of activated charcoal from dirty coal as an adsorbent for Mn (II) and Ag (I) metal ions. *Jurnal Pendidikan Kimia* 7(2):40-48 (*in Indonesian*).

Skousen, J.-G., Ziemkiewicz, P.F. and McDonald, L.M. 2019. Acid mine drainage formation, control and treatment: Approaches and strategies. *Extractive Industries and Society* 6(1):241-249, doi:10.1016/j.exis.2018.09.008.

Suliestyah, Hartami, P.N. and Tuheteru, E.J. 2020a. Effect of weight and contact time adsorption of activated carbon from coal as adsorbent of Cu(II) and Fe(II) in liquid solutions. *AIP Conference Proceedings* 2245(July), doi:10.1063/5.0007891.

Suliestyah, Hartami, N.P., Tuhuteru, E.J. and Permata, I.P. 2020b. Treatment of acid mine drainage experiment using coal-based activated carbon. *Technology Reports of Kansai University* 62(03):593-603.

CC BY-NC 4.0 | Attribution-NonCommercial 4.0 International

Suliestyah, Tuheteru, E.J., Sari, I.P. and Fajar, M.W. 2021a. Effectiveness of carbon active processed from coal in treating the acid mine drainage at a laboratory scale. *IOP Conference Series: Earth and Environmental Science* 882(1):1-7, doi:10.1088/1755-1315/882/1/012066.

Suliestyah, Hartami, N.P., Sari, I.P. and Alexander, E. 2021b. The Fe (II) and Mn (II) adsorption in acid mine drainage using various granular sizes of activated carbon and temperatures. *IOP Conference Series: Earth and Environmental Science* 882(1):1-7, doi:10.1088/1755-1315/882/1/012065.

Sun, K. and Jiang, J.C. 2010. Preparation and characterization of activated carbon from rubber-seed shell by physical activation with steam. *Biomass and Bioenergy* 34(4):539-544, doi:10.1016/j.biombioe.2009.12.020.

Sun, Y., Li, H., Li, G., Gao, B., Yue, Q. and Li, X. 2016. Characterization and ciprofloxacin adsorption properties of activated carbons prepared from biomass wastes by H_3PO_4 activation. *Bioresource Technology*217:239-244 doi:10.1016/j.biortech.2016.03.047.

Verayana, V., Paputungan, M. and Iyabu, H. 2018. The effect of HCl and H_3PO_4 activators on the characteristics (pore morphology) of coconut shell activated charcoal as well as adsorption tests on lead metal (Pb). *Jambura Journal of Educational Chemistry* 13(1):67-75 (*in Indonesian*).

Wirasnita, R., Hadibarata, T., Yusoff, A.R.M. and Lazim, M.Z. 2015. Preparation and characterization of activated carbon from oil palm empty fruit bunch wastes using zinc chloride. *Jurnal Teknologi* 74(11):77-81, doi:10.11113/jt.v74.4876.

Yagmur, E., Gokce, Y., Tekin, S., Semerci, N.I. and Aktas, Z. 2020. Characteristics and comparison of activated carbons prepared from oleaster (*Elaeagnus angustifolia* L.) fruit using KOH and ZnCl*2*. *Fuel* 267(January), doi:10.1016/j.fuel.2020.117232.

Yunus, Z.M., Othman, N., Hamdan, R. and Ruslan, N.N. 2015. Characterization of phosphoric acid impregnated activated carbon produced from honeydew peel. *Jurnal Teknologi* 76(5):15-19, doi:10.11113/jt.v76.5526.

CC BY-NC 4.0 | Attribution-NonCommercial 4.0 International

Production of activated carbon from coal with H3PO4 activation for adsorption of Fe(II) and Mn(II) in acid mine drainage

by Christin FTKE

Submission date: 03-Apr-2024 12:53PM (UTC+0700)
Submission ID: 2193340861
File name: Paper_Journal_DLML_Vol_11_No_3_2024.pdf (774.54K)
Word count: 7017
Character count: 34152

JOURNAL OF DEGRADED AND MINING LANDS MANAGEMENT
Volume 11, Number 3 (April 2024):5755-5765, doi:10.15243/jdmlm.2024.113.5755
ISSN: 2339-076X (p); 2502-2458 (e), www.jdmlm.ub.ac.id

Research Article

Production of activated carbon from coal with H_3PO_4 activation for adsorption of Fe(II) and Mn(II) in acid mine drainage

Suliestyah[1], Edy Jamal Tuheteru[1*], Ririn Yulianti[1], Christin Palit[1], Caroline Cludia Yomaki[1], Shahrul Nizam Ahmad[2]

[1] Department of Mining Engineering, Faculty of Earth and Energy Technology, Universitas Trisakti, Jl. Kyai Tapa, No. 1, Jakarta Barat 11440, Indonesia
[2] School of Chemistry and Environment, Faculty of Applied Sciences, Universiti Teknologi MARA, Shah Alam, Selangor, Malaysia

*corresponding author: ejtuheteru@trisakti.ac.id

Article history:
Received 26 September 2023
Revised 5 February 2024
Accepted 18 February 2024

Keywords:
acid mine drainage
activated carbon
adsorption
carbonization
iodine number

Abstract

Acid Mine Drainage (AMD) contains Fe(II) and Mn(II) metals, which can cause environmental pollution. This research aimed to investigate the potency of activated carbon made from coal as an adsorbent in AMD treatment. The carbon was made of coal and activated with H_3PO_4 in a weight ratio of 40%, 800°C for 120 minutes while supplying 1.5 L/min of nitrogen during the carbonization process. The result shows that BET surface area, total pore volume, and iodine number were 296.4 m^2/g, 0.156 cc/g, and 1,205 mg/g, respectively. The surface contained many fractures, channels, and big holes, as evidenced by the FT-IR and SEM investigations, and it also had acidic surface functional groups. The optimum contact time adsorption for AMD treatment was 30 minutes, and the first concentration of Fe(II) and Mn(II) metals affected the adsorption. The optimum removal of Fe(II) in AMD treatment was 95.27% at an initial concentration of 3.51 ppm, while the optimum removal of Mn(II) was 99.82% at an initial concentration of 5.71 ppm. This activated carbon has a considerable potency to be used as the adsorbent in AMD treatment to reduce Fe(II) and Mn(II) levels.

To cite this article: Suliestyah, Tuheteru, E.J., Yulianti, R., Palit, C., Yomaki, C.C. and Ahmad, S.N. 2024. Production of activated carbon from coal with H_3PO_4 activation for adsorption of Fe(II) and Mn(II) in acid mine drainage. Journal of Degraded and Mining Lands Management 11(3):5755-5765, doi:10.15243/jdmlm.2024.113.5755.

Introduction

The acid mine drainage (AMD) that is formed can have an impact on physical, chemical, biological, ecological, and socio-economic conditions. AMD has a pH range of 2 to 5 and can result from coal mining activities such as removing overburden, coal excavation, and material washing because water and oxygen present cause sulfide minerals to oxidize into sulfuric acid (Kefeni et al., 2017; Skousen et al., 2019). Besides having a low pH, AMD contains heavy metal ions such as Fe, Mn, Cd, Co, Zn, and Ni due to the interaction of AMD with various types of mineral ores (Akcil and Koldas, 2006; Garcia-Valero et al., 2020). Under chemical conditions, there is an increase in heavy metals in surface water and groundwater (Acharya and Kharel, 2020). AMD that is directly discharged into the environment can cause water pollution, corrosion of mining equipment, and damage the balance of aquatic ecosystems (Indra et al., 2014). This pollution condition can have a bad impact on the surrounding environment if AMD is not managed properly. Actions to prevent the formation of AMD have been attempted, one of which is the application of encapsulation. However, the formation of AMD cannot be avoided, so efforts need to be made to treat AMD in various forms, both through active and passive processing (Nishimoto et al., 2021).

CC BY-NC 4.0 | Attribution-NonCommercial 4.0 International

This research was carried out on a laboratory scale to see the potential for AMD treatment by using activated carbon adsorbents to minimize the impact of AMD on the surrounding environment, especially on land around the mining area.

Various methods have been carried out in processing AMD to meet the standard of mine waste, where the pH is between 6 and 8, the TSS content is ≤200 ppm, the Fe(II) metal content is ≤7 ppm and the Mn(II) metal content is ≤4 ppm (Regulation of the Ministry of Environment no 113, 2003). A method to reduce Fe(II) and Mn(II) metals in AMD waste is the use of adsorbents such as activated carbon, which has a large surface area, a regular pore structure, and functional groups on the surface, allowing the adsorption process (Kaur et al., 2018). Numerous raw materials with high carbon content can be used to produce activated carbon, namely coconut shells (Jibril et al., 2013; Liang et al., 2020), palm shells (Ibrahim et al., 2014), coffee grounds (Pagalan et al., 2019), oleaster (Yagmur et al., 2020), biomass (Abioye and Ani, 2017; Ahmed et al., 2019), rubber seed shell (Sun and Jiang, 2010), sawdust (Intan et al., 2016), fluted pumpkin stem waste (Ekpete and Horsfall, 2011), peanut shells and rice husk (Ragunita and Nandiyanto, 2021), honeydew peel (Yunus et al., 2015), oil palm empty fruit bunch wastes (Wirasnita et al., 2015) and candlenut shell (Nandiyanto et al., 2023). However, the resources are limited, which renders it difficult to meet the need to synthesize activated carbon at an industrial scale.

The use of low-rank coal, having abundant and easily accessible reserves, is required to get the activated carbon with high adsorption properties that can be applied on an industrial scale. The activated carbon from the coal has been produced using various activation and surface modification techniques and has been applied as an adsorbent. Monika (2017) has made activated carbon from coal by activating a mixture of KOH and NaOH to adsorb CO gas. Anbia and Amirmahmoodi (2016) modified the surface of coal-activated carbon using surfactants to adsorb Hg and Mn(II) metals. Coal has been used in the production of activated carbon by Li et al. (2018) and Li et al. (2020), which produces highly effective Fe(II) dye adsorbent.

The activated carbon made from coal has the potency to be adsorbent in AMD processing to reduce Fe(II) and Mn(II) levels of metals. The carbon itself has been activated using $ZnCl_2$, and its application in liquid waste can adsorb Fe(II) metal by 96% (Suliestyah et al., 2020a). The adsorption of coal-activated carbon with $ZnCl_2$ activation on Fe(II) and Mn(II) metals in AMD has been carried out, which resulted in the adsorption of 99.7-100% Fe(II) and 26.5–56 Mn(II)% (Suliestyah et al., 2020b), (Suliestyah et al., 2021a). The results showed that coal-activated carbon has a high adsorption capacity for Fe(II) metal but is still low for Mn(II) metal. Thus, it is necessary to explore alternative methods, such as the H_3PO_4 activation method, to improve the ability of the activated carbon to adsorb the Mn(II) metal.

The production of activated carbon from coal by activating a mixture of H_3PO_4 and NH_4HCO_3 has been carried out by Kusdarini et al. (2022), which produced a highly effective adsorbent with an iodine number of 1,238.5 mg/g. The production of activated carbon from coal by activating H_3PO_4 has been carried out by Sitorus (2015). The resulting activated carbon can adsorb 38.78% Mn(II) metal in artificial AMD with an initial concentration of 25 ppm at pH 3. The activation of H_3PO_4 in the process of making activated carbon has also been carried out by Esterlita and Herlina (2015), which produces activated carbon with an iodine number of 767.745 mg/g, and Sun et al. (2016), which produced activated carbon with a surface area of 1,252 m^2/g. The object of this study was the manufacture of activated carbon with coal as raw material, using phosphoric acid for activation. The resulting activated carbon was used as an adsorbent to reduce Fe and Mn metal levels in laboratory-scale acid mine drainage (AMD) treatment.

Materials and Methods

In this research, the production of activated carbon from coal was carried out using H_3PO_4 activation, a mixture of 60% coal and 40% H_3PO_4. The resulting carbon was applied as an adsorbent to Fe(II) and Mn(II) metals in artificial AMD, with the aim of seeing its potential in AMD treatment. Characterization of the activated carbon included proximate quality, iodine number, surface area, surface morphology, and infrared absorption of functional groups on the surface of activated carbon. Laboratory-scale applications used artificial AMD to carry out adsorption tests on Fe(II) and Mn(II) metals.

The coal samples were brought from PT Bukit Asam, Bangko Barat Mining Pit 1 Layer A2 Tanjung Enim, South Sumatra, Indonesia. To remove any moisture that might have been retained during the storage procedure, coal samples that had been prepared to 60 mesh size were put in a drying oven at 105°C for one hour. The samples were chemically activated using 60% coal and 40% H_3PO_4. Afterward, the samples were heated to 800°C in an airtight reactor with nitrogen flowing through it at a rate of 1.5 liters per minute for one hour in order to carbonize them. Next, hot water was used to wash and then dry the activated carbon. The choice of phosphoric acid activator is because this compound has high thermal stability and covalent character, so it is expected to increase adsorption and maximize activated carbon's potential as an adsorbent. This phosphoric acid functions to bind non-carbon impurity compounds so that the pores on the carbon will be more open (Lestari et al., 2016).

Artificial AMD was made from standard solutions containing 1,000 ppm Fe(II) and 1,000 ppm Mn(II). Each solution was diluted with distilled water,

CC BY-NC 4.0 | Attribution-NonCommercial 4.0 International

and the dilution results for two concentration variations of each solution were mixed and measured by applying AAS method for setting the concentration of Fe(II) and Mn(II); this solution was an artificial AMD. AMD samples were taken from the coal mining site of PT Banjarsari Pribumi, in the Banjarsari area, Lahat Regency, South Sumatra, Indonesia. Coal samples were taken from the mining site at Bangko Barat Mining, PT Bukit Asam, Tanjung Enim, South Sumatra, Indonesia.

In the process of characterizing activated carbon, a scanning electron microscope was used for analyzing the surface morphology (SEM- Jeol JSM-IT300), and using the Surface Area Analyzer (SAA) and Brunauer-Emmett-Teller (BET) technique, surface area, pore volume, and pore diameter were investigated. The surface's functional groups were identified using the Fourier-Transform Infrared Spectroscopy (FT-IR) method. The results of testing for Fe(II) and Mn(II) levels, both before and after activated carbon treatment, were carried out using the Atomic Absorption Spectroscopy (AAS) method. The proximate analysis included moisture content (ASTM D.3173), ash content (ASTM D.3174), volatile matter content (ASTM D.3175), and bound carbon (ASTM D.3172). Meanwhile, the sulfur content used the ASTM D.3177 method, and the calorific value used the ASTM D.5685 method.

Adsorption capacity was measured by the iodine number. Utilizing the activated carbon that had been baked in an oven, weighted up to 0.5 g, and placed in an erlenmeyer, the amount of iodine that could be adsorbed was determined. Iodine 0.1 N solution of 50 mL was applied to the sample, which was then left for 15 minutes while being shaken. Then, 10 mL of the filtrate was collected and titrated with a 0.1 N $Na_2S_2O_3$ solution. The iodine number was determined using ASTM D4607-94 method.

Activated carbon adsorption testing was carried out on a laboratory scale using artificial AMD and AMD samples taken from coal mining sites. Two grams of activated carbon were combined with 200 mL of artificial AMD and AMD samples in a different container. Then, this mixture is put into a shaker that is set to 150 rpm and 25°C. The contact time used could be anywhere between 30, 60, 90, 120, and 150 minutes. The study examined how contact time affects the elimination of the metals Fe(II) and Mn(II). The AAS was used to compare the concentration of metal ions in AMD before and after adsorption in order to assess the ability of activated carbon to get rid of Fe(II) and Mn(II) ions.

The quality of the coal used as a raw material was assessed. Table 1 shows the results of the proximate analysis, calorific value, and sulfur. Based on the finding in Table 1, the coal used to make activated carbon has Sub-Bituminous B quality.

Based on the result of dilution in the standard Fe(II) and Mn(II) solutions, two initial concentrations were obtained, which can be seen in Table 2, which shows the initial concentration in artificial AMD before treatment using activated carbon.

Table 1. Results of the analysis of coal quality.

No	Analysis Parameters	Analysis Results
1	Moisture (%, adb)	12.85
2	Ash (%, adb)	1.305
3	Volatile Matter (%, adb)	41.7256
4	Fixed Carbon (%, adb)	44.1194
5	Total Sulfur (%, adb)	0.095
6	Calorific Value (cal/g, adb)	5,445.06

Table 2. Initial concentrations of Fe(II) and Mn(II).

No	Concentration	Sample 1	Sample 2
1	Fe(II)	18.88	38.11
2	Mn(II)	11.00	18.77

From the coal mining site of PT Banjarsari Pribumi, in the Banjarsari area, Lahat Regency, South Sumatra Indonesia, the initial concentration of Fe(II) and Mn(II) is presented in Table 3.

Table 3. Initial concentrations of Fe(II) and Mn(II) from the coal mining site.

No	Fe(II) and Mn(II)	Concentration (ppm)
1	Fe(II)	3.51
2	Mn(II)	5.71

Result and Discussion

The iodine number is a parameter that shows the adsorption capacity of the activated carbon with an increase in pore size and surface area. New pores develop on the coal surface as a result of the carbonization process, and the activation of the acid prevents the formation of tar, which can close the pores. Phosphoric acid, which is hygroscopic, absorbs water in the coal before the carbonization process (Verayana et al., 2018). Table 4 shows the iodine number of coal, the activated carbon from coal without chemical activation, and the activated carbon from coal with H_3PO_4 activation. In Table 4, it appears that carbonization of coal can significantly increase the iodine from 310 mg/g to 1,043 mg/g, and activation of H_3PO_4 can increase the iodine from 1,043 mg/g to 1,206 mg/g. Activation with H_3PO_4 in this study resulted in a higher iodine number compared to the activated carbon made by Sun et al. (2016) (645 mg/g), Kurniawan et al. (2014) (219 mg/g) and by Yunus et al. (2015) (734-942 mg/g) which used coconut shell as raw material, and by Husin et al. (2020) (1,080 mg/g) which used durian peel as raw material. Table 5 shows a comparison between iodine number and proximate analysis compared to the quality standard of activated carbon based on SNI 06-3730-1995.

CC BY-NC 4.0 | Attribution-NonCommercial 4.0 International

Table 4. Iodine number.

No	Sample Type	Iodine Number (mg/g)
1	Coal	310
2	Activated carbon without chemical activation	1,043
3	Activated carbon with chemical activation of H_3PO_4	1,205

As shown in Table 5, the moisture, ash, and volatile matter content have decreased, compared to those in coal (Table 1), because the carbonization process at a temperature of 800°C has removed most of the moisture and volatile matter content in the coal. Table 5 shows that water content, ash content, and iodine numbers meet the standards for activated carbon as regulated in SNI 06-3730-1995. However, the volatile matter and bound carbon content do not meet this standard, for the time for carbonization is only 1 hour.

Table 5. Comparison of activated products with standards

No	Parameter	Activated carbon with H_3PO_4 activation	Quality Standard of Activated Carbon SNI 06-3730-1995
1	Moisture (%, adb)	9.1	Max 15
2	Ash (%, adb)	1.33	Max 10
3	Volatile Matter (%, adb)	30.3	Max 25
4	Fixed Carbon (%, adb)	59.3	Min 65
5	Iodine Number	1,205	750

Table 6 shows the BET surface area, total pore volume, and average pore diameter of the coal-derived activated carbons. The outcomes demonstrate its effectiveness as an activating agent to create the activated carbons with a high surface area and porosity. The activated carbons were carbonized using H_3PO_4 to improve their surface area and porous structure.

Table 6. Surface area, total volume, and pore radius.

No	Sample	Surface area (m^2/g)	Total Pore Volume (cc/g)	Average Pore Radius (Å)
1	Coal	2.78	0.004	27.32
2	Activated carbon activated by H_3PO_4	296.4	0.156	10.54

Activation with H_3PO_4 in this study resulted in a higher BET surface area compared to the activated carbon made by Husin and Hasibuan (2020) (44.3 m^2/g) and by Retno et al. (2016) (61.8 m^2/g) but lower BET surface area compared to the activated carbon made by Kurniawan et al. (2014) (386 m^2/g). Table 6 shows a noticeable increase in surface area from 2.78 m^2/g (raw material coal) to 296.4 m^2/g (activated carbon). The total pore volume also experienced a sharp increase from 0.004 cc/g (coal) to 0.156 cc/g (activated carbon). The surface area of this activated carbon is higher than that of the activated carbon made from durian peels with H_3PO_4 activation of 86.2 m^2/g (Husin and Hasibuan, 2020). The increased surface area of activated carbon is due to the activation process using H_3PO_4, which binds water to H_3PO_4, which is hygroscopic. This water binding can prevent the formation of tar during the carbonization process, so that the pores that are formed are not covered by tar. When new pores are formed, they will expand the surface of the activated carbon (Kurniawan et al., 2014).

A factor that affects the adsorbent's capacity to adsorb is the shape of the pore surface. The pores contained in activated carbon can increase adsorption because these pores are gaps that expand the surface of activated carbon. The coal and activated carbon from coal with the highest surface area were exposed to the SEM to investigate the surface morphology of the samples. The SEM images of the coal and the activated carbon are shown in Figures 1 and 2. The surface morphology of the coal and the activated carbon sample differ significantly from one another. Compared to activated carbon, the coal's surface is slightly smoother and has fewer Fe(II) cavities and fissures. According to the BET surface area value (2.8 m^2/g), it can be shown that the coal has a thick wall structure and only a small amount of porosity (Figure 1). This is because most of the pores in coal are still covered by hydrogen, tar, and other compounds consisting of ash, water, nitrogen, and sulfur. After the activation and carbonization processes, the raw material's thick wall opened up, and the result was a broader porosity in relation to the increase in surface area to 296.4 mg/g (Figure 2). Surface functional groups on the activated carbon were studied through FT-IR analysis (Figure 3). The FT-IR spectra of coal and activated carbon are displayed in Figures 1 and 2. After the activation, several of the prominent peaks seen in the coal vanished. In particular, it was found that the intensities of the 1,639-1,587/cm C–C stretching vibrations in aromatic ring bands and the 2,916-2,850/cm aliphatic C–H vibrations were decreased. This condition might have a relation to the activation-induced breakdown of cellulose, hemicellulose, and lignin in the coal. The presence of

CC BY-NC 4.0 | Attribution-NonCommercial 4.0 International

the OH stretching vibration of alcohol, phenol, or carboxylic acid is indicated by the broad and flat band at 3,300-3,400/cm. C-H stretching is represented by the faint peaks at 1,289/cm. Functional groups on the surface of this activated carbon have free electrons, allowing the bonding with metal ions to occur, thereby reducing the levels of Fe(II) and Mn(II) metals in the waste (Kiliç et al., 2012; Husin and Hasibuan, 2020).

Figure 1. SEM of coal.

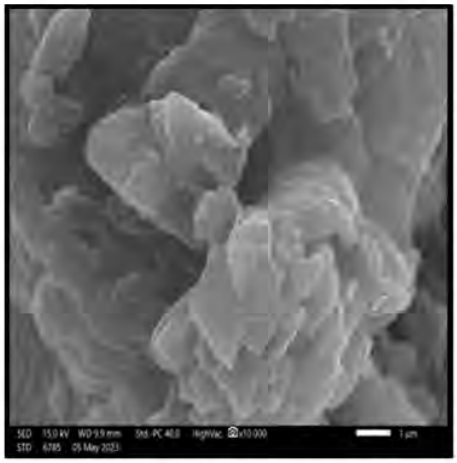

Figure 2. SEM of activated carbon.

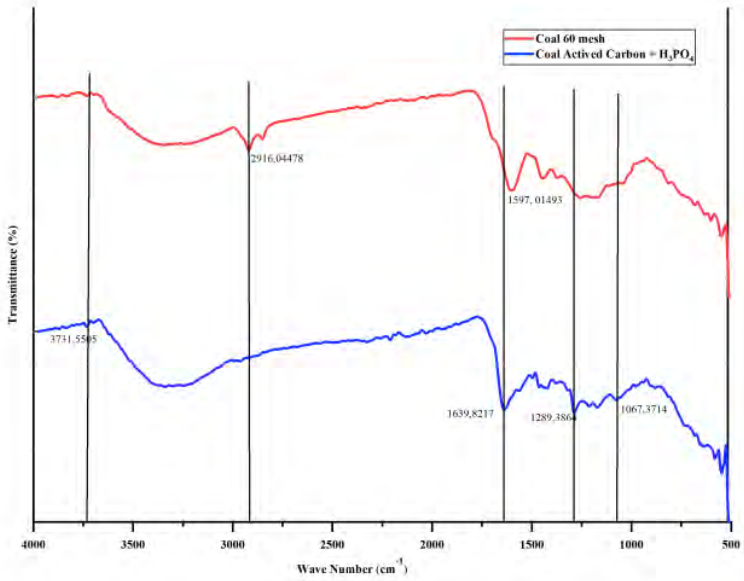

Figure 3. FT-IR of coal and activated carbon.

Table 7 shows the changes in the concentration of Fe(II) metal with initial concentrations 18.88 ppm and 38.11 ppm. Data at 0 minutes is the initial condition, and adsorption occurs at various contact times of 30, 60, 90, 120, and 150 minutes. The data in Table 7 is depicted as a graph of the reduction in Fe(II) concentration in Figure 4 and the percentage of Fe(II) uptake by activated carbon in Figure 5. Figure 4 shows that the Fe(II) removal occurs at 30 to 150 minutes. A very sharp decrease in the curve occurred at 30

CC BY-NC 4.0 | Attribution-NonCommercial 4.0 International

minutes, which showed a significant decrease in Fe(II) concentration, where at an initial concentration of 18.88 ppm, it fell to 1.15 ppm (93.9% decrease), and at an initial concentration of 38.11 ppm, it fell to 10.97 ppm (71.2% decrease). After 30 to 150 minutes, the curve appeared to be sloping, which indicated that Fe(II) removal was not significant. At an initial concentration of 18.88 ppm, the maximum removal occurred at 150 minutes at 94.9%, and for an initial concentration of 38.11 ppm, it occurred at 150 minutes at 75,29%. The percentage of Fe(II) removal is shown in Figure 5.

Table 7. The Fe(II) removal after adsorption.

Contact time of adsorption (minutes)	0	30	60	90	120	150
Concentration of sample 1 (ppm)	18.88	1.15	1.14	1.1	0.97	0.95
Concentration of sample 2 (ppm)	38.11	10.97	10.618	9.819	9.98	9.41

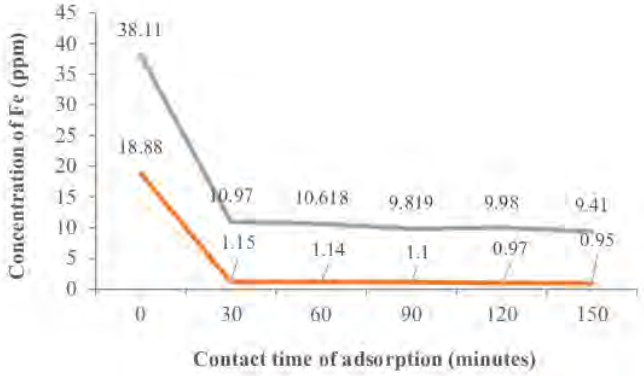

Figure 4 Reduction of Fe(II) concentration.

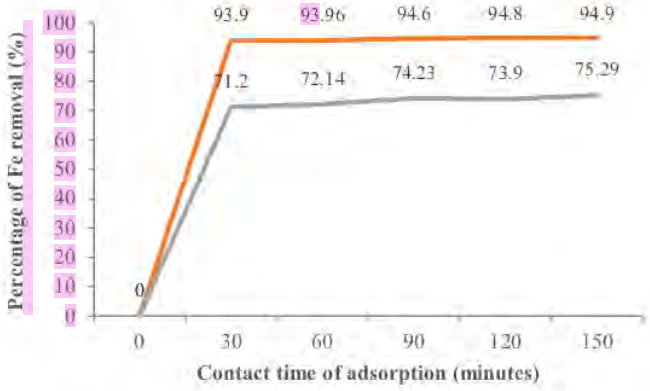

Figure 5. Percentage of Fe(II) removal.

At a lower initial concentration (18.88 ppm), the percentage of Fe(II) adsorption ranged from 93.9-94.9%, but at a higher initial concentration (38.11 ppm), the percentage of Fe(II) adsorption decreased to around 71.2-75.29%. Table 8 shows the changes in the concentration of Mn(II) metal with the initial concentrations of 11 ppm and 18.77 ppm. Data at 0 minutes is the initial condition, and adsorption occurs at various contact times of 30, 60, 90, 120, and 150 minutes. The data in Table 8 is depicted as a graph of the reduction in Mn(II) concentration in Figure 6 and the percentage of Fe(II) uptake by activated carbon in Figure 7. Figure 6 shows the concentration of Mn(II) ions in ppm units. At minute 0, the initial concentration

CC BY-NC 4.0 | Attribution-NonCommercial 4.0 International

before the adsorption of activated carbon occurs. Mn(II) removal occurs at 30 to 150 minutes. There are two curves of decreasing Mn(II) concentration with different initial concentrations. A very sharp decrease in the curve occurred at 30 minutes, which showed a significant decrease in Mn(II) concentration, in which an initial concentration at 11 ppm led to the decrease to 4.66 ppm (57.63% decrease), and at the first concentration of 18.77 ppm, it decreased into 9.51 ppm (49.26% decrease). After 30 to 150 minutes, the curve appeared to be sloping, which indicated that Mn(II) removal was not significant. At the first concentration of 11 ppm, the maximum removal occurred at 120 minutes at 65.54%. Meanwhile, for an initial concentration of 18.77 ppm, it occurred at 150 minutes at 50.38%.

Table 8. The Mn(II) removal after adsorption.

Concentration	Contact time of adsorption (minutes)					
	0	30	60	90	120	150
Concentration of sample 1 (ppm)	11	4.66	4.64	4.7164	3.7979	4.6927
Concentration of sample 2 (ppm)	18.77	9.51	9.34	9.35	9.44	9.3

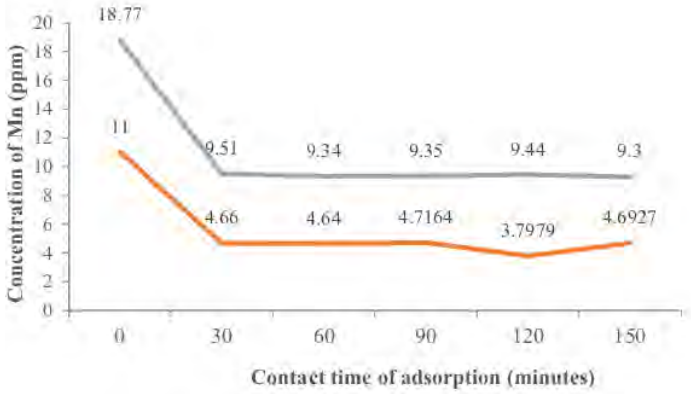

Figure 6. Reduction of Mn(II) concentration.

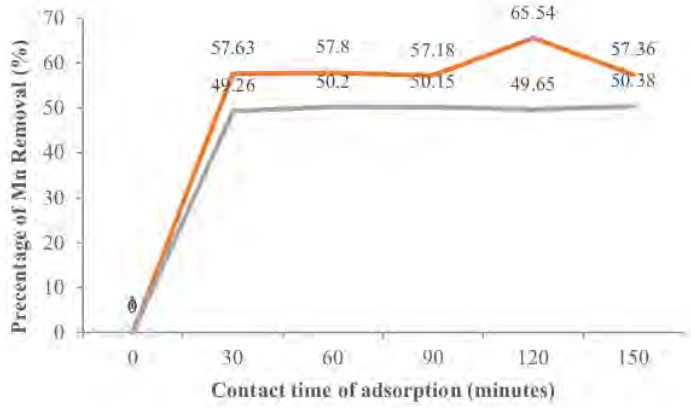

Figure 7. Percentage of Mn(II) removal.

CC BY-NC 4.0 | Attribution-NonCommercial 4.0 International

The percentage of Fe(II) removal is shown in Figure 7. The percentage of Mn(II) adsorption varied between 57.18 and 65.54% at a lower initial concentration (11 ppm) but reduced to roughly 49.26 to 50.38 percent at a higher initial concentration (18.77 ppm). This study shows that the activated carbon treatment on artificial AMD is proven effective for reducing Fe(II) and Mn(II) metals. Figures 5-7 indicate that the most effective contact time in the adsorption process was 30 minutes, which resulted in the greatest percentage of Fe(II) and Mn(II) removal. Therefore, this study continued with the activated carbon treatment on AMD samples collected from the coal mining site of PT Banjarsari Pibumu, South Sumatra (Table 9).

Table 9. The Fe(II) and Mn(II) removal after adsorption.

Concentration	Contact time (minutes)					
	0	30	60	90	120	150
Concentration of Fe(II)	3.51	0.16	0.17	0.17	0.15	0.16
Concentration of Mn(II)	5.71	0.01	0.006	0.007	0.005	0.008

Table 9 shows the changes in the concentration of Fe(II) and Mn(II) metal in the initial conditions before treatment (0 minutes) and the concentration left in AMD after adsorption by activated carbon with the contact times of 30, 60, 90, 120, and 150 minutes. The data in Table 9 is depicted as a graph of the reduced concentration of Fe(II) and Mn(II) in Figure 8 and the percentage of Fe(II) and Mn(II) uptake by activated carbon in Figure 9. Figure 8 shows the concentration of Fe(II) and Mn(II) ions in ppm units in AMD from the coal mining site. A very sharp decrease in the curve occurred at 30 minutes, which showed a significant decrease in Fe(II) concentration, where from an initial concentration of 3.51 ppm Fe(II) to 0.166 ppm (95% decrease).

At an initial Mn(II) concentration of 5.71 ppm, Fe(II) decreased to 0.01 ppm (99.8% decrease). After 30 to 150 minutes, the curve appeared to be sloping, which indicated that Fe(II) and Mn(II) removal was not significant. For Fe(II) removal, the maximum removal occurred at 120 minutes at 95.72%, and for Mn(II) removal, it occurred at 60 minutes at 99.89%. The percentage of Fe(II) and Mn(II) removal is shown in Figure 9.

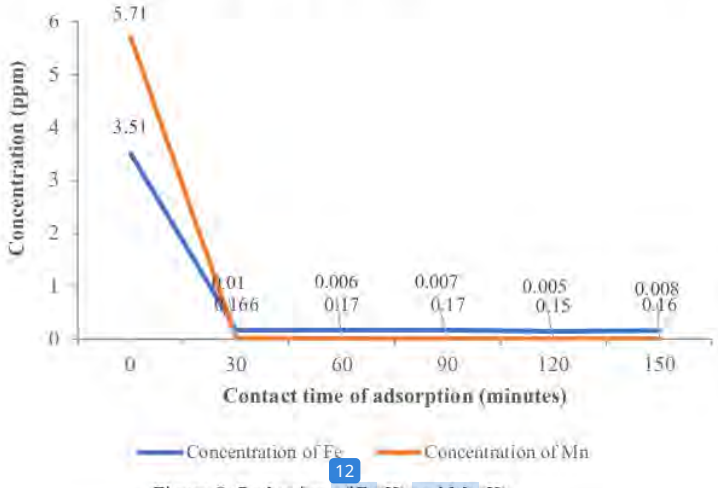

Figure 8. Reduction of Fe(II) and Mn(II).

In artificial AMD treatment with high concentrations of Fe(II) and Mn(II), the Fe(II) removal is more effective than that of Mn(II). The adsorption capacity will increase with increasing electronegativity. Because the charge on the Fe(II) ion drew more strongly toward the atomic nucleus than the Mn(II) ion did in the electron orbital, Fe(II) has a smaller ionic radius than Mn(II. The microporous nature of the activated carbon utilized makes it easier for tiny metal ions to become trapped inside its pores. Treatment of AMD from coal mining sites shows that the Fe(II) and Mn(II) removal do not differ significantly because the initial concentrations of Fe(II) and Mn(II) are low. In all AMD treatment trials with the use of activated carbon, the first concentration affected the adsorption capacity, in which higher initial concentrations of Fe and Mn led to a lower percentage of adsorption. This is because the activated carbon surface has a certain

CC BY-NC 4.0 | Attribution-NonCommercial 4.0 International

adsorption capacity for each metal. If metal adsorption has reached its maximum capacity, the adsorption process decreases. In comparison to the earlier research, which included the adsorption of Fe(II) of 85.32% (Sianipar et al., 2016), 96.24% (Suliestyah et al., 2020a), and 98.23% (Suliestyah et al., 2021b), this study produced almost the same adsorption of Fe(II) (95.7%).

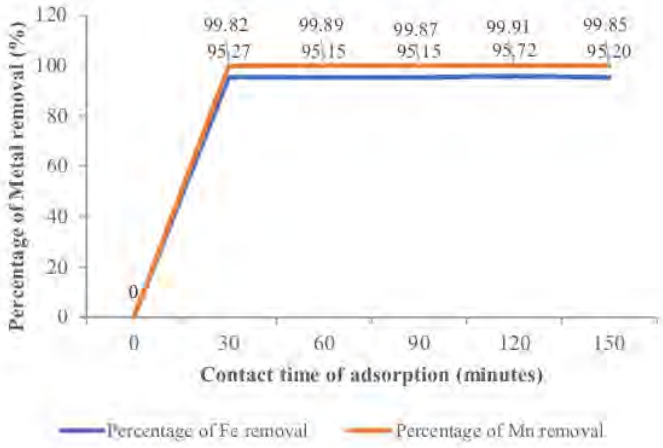

Figure 9. Percentage of Fe(II) and Mn(II).

The result of this study's Mn(II) adsorption (99.9%) was greater than that of earlier research, which reported Mn(II) absorption of 26.3% (Suliestyah et al., 2021a), 56% (Suliestyah et al., 2020b) and 92.89% (Sitorus, 2015), respectively. This study showed that the activated carbon made from coal with H_3PO_4 activation has a high adsorption capacity for Fe(II) and Mn(II) metals in artificial AMD waste, thus having a potency to be used as an adsorbent in AMD treatment.

Conclusion

The characterization of activated carbon with H_3PO_4 activation revealed that the BET surface area, total pore volume, and iodine number were 296.4 m^2/g, 0.1562 cc/g, and 1206 mg/g, respectively. The FT-IR and SEM analyses showed that the surface had acidic surface functional groups and was extremely porous, with numerous fractures, channels, and sizable holes. Treatment of activated carbon in artificial AMD showed that adsorption was affected by the initial concentration of Fe(II) and Mn(II) metals. The greater the initial concentration of Fe(II) and Mn(II), the lower the adsorption power of activated carbon. The results showed that AMD adsorption treatment using H_3PO_4 activated carbon was achieved at 30 minutes of the optimum contact time, with a percentage of Fe(II) removal of 95.27% and a percentage of Mn(II) removal of 99.82%. The findings of this study suggest that the use of coal-activated carbon with H_3PO_4 activation as an adsorbent in AMD treatment to lower Fe(II) and Mn(II) levels has a very high potential.

Acknowledgments

The authors acknowledge PT Bukit Asam for allowing coal sampling and PT Banjarsari Pribumi for allowing acid mine drainage to be sampled. Thanks are also directed to the BRIN laboratory for assisting in testing BET, SEM, FT-IR, and AAS, and to the Coal Quality Analysis Laboratory for assisting in testing the quality of coal and activated carbon.

References

Abioye, A.M. and Ani, F.N. 2017. Advancement in the production of activated carbon from biomass using microwave heating. *Jurnal Teknologi (Sciences & Engineering)* 79(3):79-88, doi:10.11113/jt.v79.7249.

Acharya, B.S. and Kharel, G. 2020. Acid mine drainage from coal mining in the United States – An overview. *Journal of Hydrology* 588(April):125061, doi:10.1016/j.jhydrol.2020.125061.

Ahmed, M.B., Hasan Johir, M.A., Zhou, J.L., Ngo, H.H., Nghiem, L.D., Richardson, C., Moni, M.A. and Bryant, M.R. 2019. Activated carbon preparation from biomass feedstock: Clean production and carbon dioxide adsorption. *Journal of Cleaner Production* 225:405-413, doi:10.1016/j.jclepro.2019.03.342.

Akcil, A. and Koldas, S. 2006. Acid Mine Drainage (AMD): causes, treatment and case studies. *Journal of Cleaner Production* 14(12-13 SPEC. ISS.):1139-1145, doi:10.1016/j.jclepro.2004.09.006.

Anbia, M. and Amirmahmoodi, S. 2016. Removal of Hg (II) and Mn (II) from aqueous solution using nanoporous carbon impregnated with surfactants. *Arabian Journal of Chemistry* 9:S319-S325, doi:10.1016/j.arabjc.2011.04.004.

Ekpete, O. and Horsfall, M. 2011. Preparation and characterization of activated carbon derived from fluted

CC BY-NC 4.0 | Attribution-NonCommercial 4.0 International

pumpkin stem waste (*Telfairia occidentalis* Hook F). *Research Journal of Chemical Sciences* 1(3):10-17.

Esterlita, M.O. and Herlina, N. 2015. Effect of adding $ZnCl_2$, KOH, and H_3PO_4 activators in making active carbon from sugar palm fronds (*Arenga pinnata*). *Jurnal Teknik Kimia USU* 4(1):47-52, doi:10.32734/jtk.v4i1.1460 (*in Indonesian*).

Garcia-Valero, A., Martínez-Martínez, S., Faz, A., Rivera, J. and Acosta, J.A. 2020. Environmentally sustainable acid mine drainage remediation: Use of natural alkaline material. *Journal of Water Process Engineering* 33(December 2019):101064, doi:10.1016/j.jwpe.2019.101064.

Husin, A. and Hasibuan, A. 2020. Study of the effect of varying phosphoric acid (H_3PO_4) concentration and carbon soaking time on the characteristics of activated carbon from durian peel. *Jurnal Teknik Kimia USU* 9(2):80-86, doi:10.32734/jtk.v9i2.3728 (*in Indonesian*).

Ibrahim, I., Martin, A. and Nasruddin, N. 2015. Manufacture and characterization of activated carbon made from palm shells using the physical activation method using a rotary autoclave. *Jom FTEKNIK* 1(2):1-11 (*in Indonesian*).

Indra, H., Lepong, Y., Gunawan, F. and Abfertiawan, M.S. 2014. Application of active and passive treatment methods in management of Lati site acid mine water. *5th Acid Mine Water and Post-mining Seminar in Indonesia*, November 2014, 1-9 (*in Indonesian*).

Intan, D., Said, I. and Abram, H. 2016. Utilization of sawdust biomass as an absorbent for lead metal. *Jurnal Akademika Kimia* 5(4):166-171 (*in Indonesian*).

Jibril, M., Noraini, J., Poh, L.S. and Evuti, A.M. 2013. Removal of colour from waste water using coconut shell activated carbon (CSAC) and commercial activated carbon (CAC). *Jurnal Teknologi (Sciences and Engineering)* 60(May 2014):15-19, doi:10.11113/jt.v60.1435.

Kaur, G., Couperthwaite, S.J., Hatton-Jones, B.W. and Millar, G.J. 2018. Alternative neutralisation materials for acid mine drainage treatment. *Journal of Water Process Engineering* 22(January):46-58, doi:10.1016/j.jwpe.2018.01.004.

Kefeni, K.K., Msagati, T.A.M. and Mamba, B.B. 2017. Acid mine drainage: Prevention, treatment options, and resource recovery: A review. *Journal of Cleaner Production* 151:475-493, doi:10.1016/j.jclepro.2017.03.082.

Kiliç, M., Apaydin-Varol, E. and Pütün, A.E. 2012. Preparation and surface characterization of activated carbons from *Euphorbia rigida* by chemical activation with $ZnCl_2$, K_2CO_3, NaOH, and H_3PO_4. *Applied Surface Science* 261:247-254, doi:10.1016/j.apsusc.2012.07.155.

Kurniawan, R., Luthfi, M. and Wahyunanto, A. 2014. Characterization of BET (Braunanear, Emmelt and Teller) surface area of activated carbon from coconut shells and empty oil palm fruit bunches with phosphoric acid activation. *Jurnal Keteknikan Pertanian Tropis dan Biosistem* 2(1):15-20 (*in Indonesian*).

Kusdarini, E., Budianto, A. and Ghafarunnisa, D. 2017. Production of activated carbon from bituminous coal with a single activation of H_3PO_4, combination of H_3PO_4-NH_4HCO_3, and thermal. *Reaktor* 17(2):74, doi:10.14710/reaktor.17.2.74-80 (*in Indonesian*).

Lestari, R.S.D., Sari, D.K., Rosmadiana, A. and Dwipermata, B. 2016. Preparation and characterization of coconut shell activated carbon with phosphoric acid activator and its application in the purification of used cooking oil. *Teknika: Jurnal Sains dan Teknologi* 12(2):419, doi:10.36055/tjst.v12i2.6607 (*in Indonesian*).

Li, H., Zheng, F., Wang, J., Zhou, J., Huang, X., Chen, L., Hu, P., Gao, J.M., Zhen, Q., Bashir, S. and Liu, J.L. 2020. Facile preparation of zeolite-activated carbon composite from coal gangue with enhanced adsorption performance. *Chemical Engineering Journal* 390, doi:10.1016/j.cej.2020.124513.

Li, L., Sun, F., Gao, J., Wang, L., Pi, X. and Zhao, G. 2018. Broadening the pore size of coal-based activated carbon: Via a washing-free chem-physical activation method for high-capacity dye adsorption. *RSC Advances* 8(26):14488-14499, doi:10.1039/c8ra02127a.

Liang, Q., Liu, Y., Chen, M., Ma, L., Yang, B., Li, L. and Liu, Q. 2020. Optimized preparation of activated carbon from coconut shell and municipal sludge. *Materials Chemistry and Physics* 241(July 2019)., doi:10.1016/j.matchemphys.2019.122327.

Monika, I. 2017. Potential study of Indonesia coal for adsorbed natural gas. *Indonesian Mining Journal* 19(3):133-142, doi:10.30556/imj.vol19.no3.2016.406.

Nandiyanto, A.B.D., Fiandini, M., Ragadhita, R. and Aziz, M. 2023. How to purify and experiment with dye adsorption using carbon: step-by-step procedure from carbon conversion from agricultural biomass to concentration measurement using UV Vis Spectroscopy. *Indonesian Journal of Science & Technology* 8:363-380.

Nishimoto, N., Yamamoto, Y., Yamagata, S., Igarashi, T. and Tomiyama, S. 2021. Acid mine drainage sources and impact on groundwater at the Osarizawa mine, Japan. *Minerals* 11(9):1-15, doi:10.3390/min11090998.

Pagalan, E., Sebron, M., Gomez, S., Salva, S.J., Ampusta, R., Macarayo, A.J., Joyno, C., Ido, A. and Arazo, R. 2019. Activated carbon from spent coffee grounds as an adsorbent for treatment of water contaminated by aniline yellow dye. *Industrial Crops and Products* 145:111953, doi:10.1016/j.indcrop.2019.111953.

Ragadhita, R. and Nandiyanto, A.B.D. 2021. How to calculate adsorption isotherms of particles using two-parameter monolayer adsorption models and equations. *Indonesian Journal of Science and Technology* 6(1):205-234, doi:10.17509/ijost.v6i1.32354.

Regulation of the Ministry of Environment no 113. 2003. Waste Water Quality Standards for Coal Mining Businesses and Activities (*in Indonesian*).

Sianipar, L.D., Zaharah, T.A. and Syahbanu, I. 2016. Adsorption of Fe(II) with cocoa (*Theobroma cacao* L.) fruit shell charcoal activated by hydrochloric acid. *Jurnal Kimia Khatulistiwa* 5(2):50-59 (*in Indonesian*).

Sitorus, S. 2015. Utilization of activated charcoal from dirty coal as an adsorbent for Mn (II) and Ag (I) metal ions. *Jurnal Pendidikan Kimia* 7(2):40-48 (*in Indonesian*).

Skousen, J.-G., Ziemkiewicz, P.F. and McDonald, L.M. 2019. Acid mine drainage formation, control and treatment: Approaches and strategies. *Extractive Industries and Society* 6(1):241-249, doi:10.1016/j.exis.2018.09.008.

Suliestyah, Hartami, P.N. and Tuheteru, E.J. 2020a. Effect of weight and contact time adsorption of activated carbon from coal as adsorbent of Cu(II) and Fe(II) in liquid solutions. *AIP Conference Proceedings* 2245(July), doi:10.1063/5.0007891.

Suliestyah, Hartami, N.P., Tuhuteru, E.J. and Permata, I.P. 2020b. Treatment of acid mine drainage experiment using coal-based activated carbon. *Technology Reports of Kansai University* 62(03):593-603.

CC BY-NC 4.0 | Attribution-NonCommercial 4.0 International

Suliestyah, Tuheteru, E.J., Sari, I.P. and Fajar, M.W. 2021a. Effectiveness of carbon active processed from coal in treating the acid mine drainage at a laboratory scale. *IOP Conference Series: Earth and Environmental Science* 882(1):1-7, doi:10.1088/1755-1315/882/1/012066.

Suliestyah, Hartami, N.P., Sari, I.P. and Alexander, E. 2021b. The Fe (II) and Mn (II) adsorption in acid mine drainage using various granular sizes of activated carbon and temperatures. *IOP Conference Series: Earth and Environmental Science* 882(1):1-7, doi:10.1088/1755-1315/882/1/012065.

Sun, K. and Jiang, J.C. 2010. Preparation and characterization of activated carbon from rubber-seed shell by physical activation with steam. *Biomass and Bioenergy* 34(4):539-544, doi:10.1016/j.biombioe.2009.12.020.

Sun, Y., Li, H., Li, G., Gao, B., Yue, Q. and Li, X. 2016. Characterization and ciprofloxacin adsorption properties of activated carbons prepared from biomass wastes by H_3PO_4 activation. *Bioresource Technology* 217:239-244 doi:10.1016/j.biortech.2016.03.047.

Verayana, V., Paputungan, M. and Iyabu, H. 2018. The effect of HCl and H_3PO_4 activators on the characteristics (pore morphology) of coconut shell activated charcoal as well as adsorption tests on lead metal (Pb). *Jambura Journal of Educational Chemistry* 13(1):67-75 (*in Indonesian*).

Wirasnita, R., Hadibarata, T., Yusoff, A.R.M. and Lazim, M.Z. 2015. Preparation and characterization of activated carbon from oil palm empty fruit bunch wastes using zinc chloride. *Jurnal Teknologi* 74(11):77-81, doi:10.11113/jt.v74.4876.

Yagmur, E., Gokce, Y., Tekin, S., Semerci, N.I. and Aktas, Z. 2020. Characteristics and comparison of activated carbons prepared from oleaster (*Elaeagnus angustifolia* L.) fruit using KOH and $ZnCl_2$. *Fuel* 267(January), doi:10.1016/j.fuel.2020.117232.

Yunus, Z.M., Othman, N., Hamdan, R. and Ruslan, N.N. 2015. Characterization of phosphoric acid impregnated activated carbon produced from honeydew peel. *Jurnal Teknologi* 76(5):15-19, doi:10.11113/jt.v76.5526.

CC BY-NC 4.0 | Attribution-NonCommercial 4.0 International

Production of activated carbon from coal with H3PO4 activation for adsorption of Fe(II) and Mn(II) in acid mine drainage

ORIGINALITY REPORT

20%	16%	15%	5%
SIMILARITY INDEX	INTERNET SOURCES	PUBLICATIONS	STUDENT PAPERS

PRIMARY SOURCES

1	doaj.org Internet Source	7%
2	www.karyailmiah.trisakti.ac.id Internet Source	2%
3	repository.unibos.ac.id Internet Source	2%
4	Khalid Z. Elwakeel, Gamal O. El-Sayed, Susan M. Abo El-Nassr. "Removal of ferrous and manganous from water by activated carbon obtained from sugarcane bagasse", Desalination and Water Treatment, 2014 Publication	1%
5	www.researchgate.net Internet Source	1%
6	Ying Zhang, Jiaying Zhao, Zhao Jiang, Dexin Shan, Yan Lu. "Biosorption of Fe(II) and Mn(II) Ions from Aqueous Solution by Rice Husk Ash", BioMed Research International, 2014 Publication	1%

7	Zhao Jiang, Bo Cao, Guangxia Su, Yan Lu, Jiaying Zhao, Dexin Shan, Xiuyuan Zhang, Ziyi Wang, Ying Zhang. " Comparison on the Surface Structure Properties along with Fe(II) and Mn(II) Removal Characteristics of Rice Husk Ash, Inactive Powder, and Rice Husk ", BioMed Research International, 2016 Publication	1 %
8	www.science.gov Internet Source	1 %
9	Suliestyah, A D Astuti, I P Sari. "Utilization of lignite coal as heavy metal adsorbent in chemistry laboratory wastewater", IOP Conference Series: Earth and Environmental Science, 2021 Publication	1 %
10	jdmlm.ub.ac.id Internet Source	1 %
11	Submitted to Rudarsko-geološko-naftni fakultet / Faculty of Mining, Geology and Petroleum Engineering Student Paper	<1 %
12	repo-dosen.ulm.ac.id Internet Source	<1 %
13	Cut Nursiah, Hera Desvita, Elviani Elviani, Nurlia Farida et al. "Adsorbent	<1 %

Characterization from Cocoa Shell Pyrolysis (*Theobroma cacao* L) and Its Application in Mercury Ion Reduction", Journal of Ecological Engineering, 2023
Publication

14	iaeme.com Internet Source	<1%
15	Haimour, N.M.. "Utilization of date stones for production of activated carbon using phosphoric acid", Waste Management, 2006 Publication	<1%
16	Sulistyani, S Kristianingrum, E D Siswani, A Fillaeli. " Identification of activated NaOH carbon of synthesis of sea pandanus leaves (.) for Fe and Cu ions adsorption ", Journal of Physics: Conference Series, 2019 Publication	<1%
17	Shaohua Lin, Huijun He, Rui Zhang, Jierui Li. "Removal of Fe (II) and Mn (II) from Aqueous Solution by Palygorskite", 2011 International Conference on Computer Distributed Control and Intelligent Environmental Monitoring, 2011 Publication	<1%
18	www.journal.ugm.ac.id Internet Source	<1%

19	Seong-Jik Park, Chang-Gu Lee, Jae-Hyun Kim, Song-Bae Kim, Yoon-Young Chang, Jae-Kyu Yang. "Bimetallic oxide-coated sand filter for simultaneous removal of bacteria, Fe(II), and Mn(II) in small- and pilot-scale column experiments", Desalination and Water Treatment, 2014 Publication	<1 %
20	Submitted to Sriwijaya University Student Paper	<1 %
21	Submitted to State Islamic University of Alauddin Makassar Student Paper	<1 %
22	docplayer.info Internet Source	<1 %
23	Biomass and Bioenergy, 2014. Publication	<1 %
24	Murat Kılıç, Esin Apaydın-Varol, Ayşe Eren Pütün. "Preparation and surface characterization of activated carbons from Euphorbia rigida by chemical activation with ZnCl2, K2CO3, NaOH and H3PO4", Applied Surface Science, 2012 Publication	<1 %
25	Zhu, Chi, Shui Wang, Kai Ming Hu, Wei Xia Wang, An Juan Cai, Wen Jie Chang, and Bing Li. "Study on Fluoride, Iron and Manganese	<1 %

Removal from Aqueous Solutions by a Novel Composite Adsorbent", Advanced Materials Research, 2013.

Publication

Exclude quotes	On	Exclude matches	< 15 words
Exclude bibliography	On		